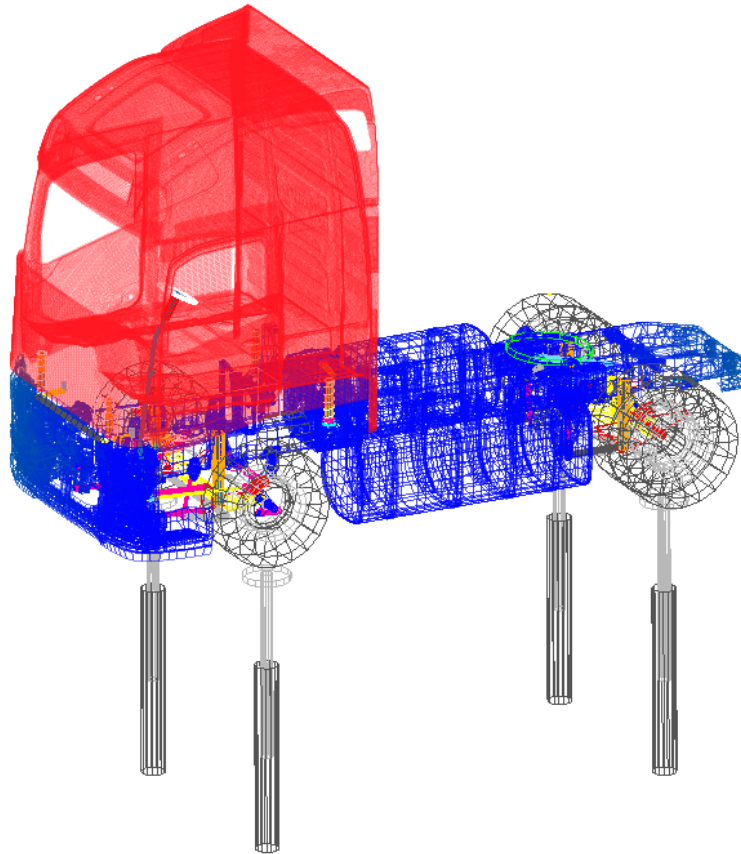


CHALMERS



Design and simulation of active and semi-active cab suspensions with focus to improve ride comfort of a heavy truck

Master's thesis in Applied Mechanics

CHRISTINE EKBERG
ERIK HANSSON

Department of Applied Mechanics
Division of Dynamics
CHALMERS UNIVERSITY OF TECHNOLOGY
Gothenburg, Sweden 2015
Master's thesis 2015:21

MASTER'S THESIS IN APPLIED MECHANICS

Design and simulation of active and semi-active cab
suspensions with focus to improve ride comfort of a heavy truck

CHRISTINE EKBERG
ERIK HANSSON

Department of Applied Mechanics
Division of Dynamics
CHALMERS UNIVERSITY OF TECHNOLOGY
Gothenburg, Sweden 2015

Design and simulation of active and semi-active cab
suspensions with focus to improve ride comfort of a heavy truck
CHRISTINE EKBERG
ERIK HANSSON

© CHRISTINE EKBERG, ERIK HANSSON, 2015

Master's thesis 2015:21
ISSN 1652-8557
Department of Applied Mechanics
Division of Dynamics
Chalmers University of Technology
SE-412 96 Gothenburg
Sweden
Telephone: +46 (0)31-772 1000

Cover:
Adams model of a Volvo FH tractor in a four-post test rig simulation of complete vehicle

Chalmers Reproservice
Gothenburg, Sweden 2015

Design and simulation of active and semi-active cab
suspensions with focus to improve ride comfort of a heavy truck
Master's thesis in Applied Mechanics
CHRISTINE EKBERG
ERIK HANSSON
Department of Applied Mechanics
Division of Dynamics
Chalmers University of Technology

ABSTRACT

Ride comfort is strongly related to the vibrations a driver experience. Truck drivers are exposed to vibrations all day as part of their work, which makes ride comfort an important vehicle feature. The vibrations can cause motion related injuries, which not only affect the driver's health but also have a large impact on the national economy. Constant vibrations can also lead to fatigue of the driver, which in turn can have safety implications. Another key safety factor when operating a commercial truck is vehicle handling. Both ride comfort and handling are highly influenced by the cab suspension. A conventional cab suspension is comprised by a spring and passive damper combination. Good ride comfort is generally achieved by a rather soft suspension setting while a rather hard setting provides good handling. Consequently, the aim to have both good ride comfort and handling is often contradictory. The goal of this thesis is to improve ride comfort while maintaining good handling features, through the use of active and semi-active cab suspensions. The focus of the study is the vertical dampers, which are positioned in the corners in the front and the rear of the cab.

Studies have shown that ride comfort can be improved through the use of active and semi-active cab suspensions. The technology can already be found in passenger cars and the truck industry has begun to approach this solution for the cab suspension as well. Previous available research mainly addresses simplified models of the cab but complete vehicle models with active and semi-active cab suspensions have not yet been studied to the same extent.

One of the main outputs of this thesis is a method to design and implement active and semi-active cab suspensions in Adams/Car for complete vehicle analysis. The result also comprises comfort and handling analysis using different control algorithms and control strategies. The control systems are mainly based on skyhook theory, introduced by Karnopp et al in the 1970s. A control system using Linear Quadratic Regulator (LQR) control is also designed and implemented. The design and development of the control systems is done in Matlab/Simulink using a model of the cab and it's suspensions. The control algorithm is then implemented in Adams/Car and used in vehicle testing.

The main findings of this thesis satisfy the objective of the project to a large extent. The analysis of the active control systems show significant improvements in terms of increased comfort compared to the conventional passive dampers. The semi-active control systems also improve the ride comfort but the same performance is not achieved as with the active systems, as expected. Moreover, the performance of the semi-active control systems are more dependent on the road severity compared to the active systems. The handling tests mainly shows equivalent or improved handling features through the implementation of active and semi-active controllers. The only drawback is an increased time delay between the driver steering input and the response, generated by the active control systems. The findings of the study provide good prerequisites for future work as it highlights the behaviour of the control systems for specific conditions as well as describes a method to develop and implement control systems in full vehicle models.

Keywords: Cab suspension, ride comfort, vehicle handling, complete vehicle model, active control, semi-active control, skyhook, LQR

ACKNOWLEDGEMENTS

We would like to acknowledge and thank our mentors, Andreas Gustavsson and Anders Lindström, who have provided with their technical knowledge to help us complete this project. We would also like to thank the rest of the team at the department of Chassis Strategy & Vehicle analysis at Volvo Group Trucks Technology for their hospitality during our project work. Additionally, we would like to thank our examiner, Viktor Berbyuk at the Dynamics division of the department of Applied Mechanics, for the help and support through the project.

NOMENCLATURE

| | |
|--------------|--|
| Q | Weighting matrix states |
| R | Weighting matrix forces |
| u | External input forces |
| x | State vector of the cab |
| θ_x | Roll angle of the cab |
| θ_y | Pitch angle of the cab |
| a_v | 3D-value for weighted acceleration |
| $a_{rms,wi}$ | Weighted rms value in x-,y- or z-direction |
| c_{heave} | Skyhook heave damping coefficient |
| c_{pitch} | Skyhook pitch damping coefficient |
| c_{roll} | Skyhook roll damping coefficient |
| c_{sky} | Skyhook damping coefficient |
| F_{sa} | Semi-active control force |
| F_{sky} | Skyhook force |
| J_x | Moment of inertia around the roll axes for the cab |
| J_y | Moment of inertia around the pitch axes for the cab |
| k_x | Rms value weight in x-direction |
| k_y | Rms value weight in y-direction |
| k_z | Rms value weight in z-direction |
| LQR | Linear Quadratic Regulator |
| m | Mass of the cab |
| u_{fl} | Lower position of the suspension, front left |
| u_{fr} | Lower position of the suspension, front right |
| u_{rl} | Lower position of the suspension, rear left |
| u_{rr} | Lower position of the suspension, rear right |
| v_0 | No-jerk tuning parameter |
| v_{rel} | Relative velocity in the suspension point |
| $W_{d,AVT}$ | Acceleration velocity transition filter, horizontal sensitivity function |
| $W_{d,HP}$ | High pass filter, horizontal sensitivity function |
| $W_{d,LP}$ | Low pass filter, horizontal sensitivity function |
| $W_{d,UP}$ | Upward step filter, horizontal sensitivity function |
| $W_{k,AVT}$ | Acceleration velocity transition filter, vertical sensitivity function |
| $W_{k,HP}$ | High pass filter, vertical sensitivity function |
| $W_{k,LP}$ | Low pass filter, vertical sensitivity function |
| $W_{k,UP}$ | Upward step filter, vertical sensitivity function |
| z | Heave position of the cab |

| | |
|----------|--|
| z_{fl} | The z-coordinate of the cab, front left |
| z_{fr} | The z-coordinate of the cab, front right |
| z_{rl} | The z-coordinate of the cab, rear left |
| z_{rr} | The z-coordinate of the cab, rear right |

CONTENTS

| | |
|--|------------|
| Abstract | i |
| Acknowledgements | i |
| Nomenclature | iii |
| Contents | v |
| 1 Introduction | 1 |
| 1.1 Background | 1 |
| 1.2 Purpose | 2 |
| 1.3 Limitations | 2 |
| 1.4 Report outline | 2 |
| 2 Theory | 5 |
| 2.1 The truck | 5 |
| 2.1.1 Cab suspension | 6 |
| 2.1.2 Truck model | 6 |
| 2.2 Comfort | 7 |
| 2.2.1 Ride comfort analysis | 7 |
| 2.2.2 Vibrations and the human body | 8 |
| 2.3 Handling | 11 |
| 2.3.1 Handling analysis | 11 |
| 2.4 Cab model | 12 |
| 2.4.1 Estimating the modal coordinates | 15 |
| 2.4.2 Modal force distribution | 15 |
| 2.5 Passive vibration control | 16 |
| 2.5.1 Undamped system | 17 |
| 2.5.2 Underdamped system | 17 |
| 2.5.3 Critically damped system | 17 |
| 2.5.4 Overdamped system | 17 |
| 2.5.5 Characteristic response | 18 |
| 2.6 Active vibration control | 18 |
| 2.6.1 Individual Skyhook | 19 |
| 2.6.2 Modal Skyhook | 19 |
| 2.6.3 Linear Quadratic Regulator | 19 |
| 2.7 Semi-active vibration control | 21 |

| | | |
|----------|---|-----------|
| 2.7.1 | Semi-active Individual Skyhook | 21 |
| 2.7.2 | Semi-active Modal Skyhook | 22 |
| 2.8 | No-jerk Shape Function | 22 |
| 3 | Benchmark tests | 25 |
| 3.1 | Sensitivity analysis | 25 |
| 3.2 | Comfort | 25 |
| 3.3 | Handling | 26 |
| 3.4 | Long dip | 27 |
| 4 | Controller Design | 29 |
| 4.1 | Implementation of control system | 29 |
| 4.2 | No-jerk tuning | 30 |
| 4.3 | Test cases | 30 |
| 4.3.1 | Case 1 - Active individual skyhook | 31 |
| 4.3.2 | Case 2 - Semi-active individual skyhook | 31 |
| 4.3.3 | Case 3 - Active modal skyhook | 32 |
| 4.3.4 | Case 4 - Semi-active modal skyhook | 33 |
| 4.3.5 | Case 5 - Active LQR | 34 |
| 4.3.6 | Case 6 - Long dip | 36 |
| 5 | Results | 37 |
| 5.1 | Case 1 - Active individual skyhook | 37 |
| 5.1.1 | Comfort | 37 |
| 5.1.2 | Handling | 38 |
| 5.2 | Case 2 - Semi-active individual skyhook | 40 |
| 5.2.1 | Comfort | 40 |
| 5.2.2 | Handling | 41 |
| 5.3 | Case 3 - Active modal skyhook | 42 |
| 5.3.1 | Comfort | 42 |
| 5.3.2 | Handling | 43 |
| 5.4 | Case 4 - Semi-active modal skyhook | 45 |
| 5.4.1 | Comfort | 45 |
| 5.4.2 | Handling | 46 |
| 5.5 | Case 5 - Active LQR | 47 |
| 5.5.1 | Comfort | 47 |
| 5.5.2 | Handling | 48 |
| 5.6 | Case 6 - Long dip | 48 |
| 5.6.1 | Active individual skyhook | 48 |

| | | |
|----------|--|-----------|
| 5.6.2 | Semi-active individual skyhook | 49 |
| 6 | Discussion | 51 |
| 6.1 | Comparison of active and semi-active control | 51 |
| 6.2 | Comparison of individual and modal control | 52 |
| 6.3 | Cab model | 52 |
| 6.4 | Road profiles and road obstacles | 53 |
| 6.5 | Recommendations for future work | 53 |
| 7 | Conclusions | 55 |
| | References | 57 |

1 Introduction

This report will provide a presentation of the thesis project *Design and simulation of active and semi active cab suspensions with focus to improve ride comfort of a heavy truck*. The project is conducted at the department of Applied Mechanics at Chalmers University of Technology in collaboration with Volvo Group Trucks Technology. The objective of this study is to improve ride comfort through the use of active and cab semi-active suspensions, with focus on the vertical dampers. Handling and manoeuvrability are also studied with the purpose to maintain the handling features of today's vehicles. Here follows a description of the problem and a presentation of previous research as well as the contributions of this project. The purpose of the project and the limitations are also presented.

1.1 Background

The primary suspension in a truck has the purpose to carry the load, minimize road damage, protect the chassis from shocks while providing good handling behaviour and road holding. The cab suspension, also often called the secondary suspension, connects the cab to the chassis and acts as vibration isolation system between the cab and the rest of the vehicle. When the purpose is to increase comfort by minimizing the vibrations in the cab, the cab suspension is the first place to start look for improvement opportunities.

When driving a vehicle, excitations from the road and the engine induce vibrations that affect the comfort of the driver. A major difference between passenger cars and trucks is the position of the driver. In a truck is the driver placed far above the roll and pitch centre, which increases the lateral and longitudinal motions induced by these rotations. The position of the driver is therefore not optimal for comfort issues according to Gillespie [1]. Ride comfort, handling and manoeuvrability of the vehicle are all affected by the suspension systems. While ride comfort is characterized by a rather soft setting for the springs and dampers, good road holding is provided by a rather stiff setting. In an ideal handling case, the cab follows the chassis motion without delay, giving direct feedback to the driver. The delay can partly be decreased by using very stiff anti roll bars but adding stiff parts will again be a source of discomfort for the truck driver. Consequently, the aim to have both good handling and manoeuvrability and a good comfort level is therefore often contradictory [2]. Both comfort and handling features are essential for safety as well as the driving experience. Poor handling and manoeuvrability will cause safety issues since the driver's ability to interpret input from the road is vital when driving. Additionally, constant vibration can add to the fatigue of the driver, which in turn can have implications on the safety. Constant vibrations can also result in motion injuries such as muscle and back pain. Motion related injuries for drivers in commercial vehicles have a huge impact on the economy. According to Deprez et al. [3], motion related injuries the single largest cause of industrial disability and account for 20% of all work injuries for people under 45 in the United States. This example emphasizes the importance of having good ride comfort in commercial trucks, which concerns the truck industry globally.

The potential for improvement of today's passive spring-damper suspension is limited due to constant damping and spring coefficients. Hence, to meet future feature demands of increased comfort and performance, new suspension characteristics are required. Semi-active and active suspensions have the possibility to change the characteristics over time and studies show that these suspensions can be used to improve vehicle performance. Already in 1974, Karnopp [4] discussed vibration control using active and semi-active suspensions, saying that both active and semi-active suspensions have proven advantaged compared to a passive system. However, that the increased cost and complexity of active systems only justifies substitution in cases when the performance is critical while semi-active system can provide significant performance gains for little extra cost. In a study made by Van Deusen in 1973 it was seen that ride quality for heavy trucks could be improved by softening the suspensions system [5]. A side effect of that was that the roll stiffness was affected in a negative way, resulting in variations in handling depending on how truck was loaded.

More recent studies have been made on simplified cab models with semi-active suspensions, pointing to improved performance when substituting the passive system. Fischer and Isermann [6] gave an overview in 2004 showing that semi-active suspension could reduce the vibrations by 20-30% and that an active system can reduce the vibrations with over 30%. Florin conducted a study that provided a prototype of the cab suspension and semi-active controller that were tested in a laboratory and on the road, concluding improved performance in

terms on comfort and handling [7]. However, no studies have been found describing complete vehicle analysis using active or semi-active cab suspensions, which is what this project aims to do. A model with an integrated control system enables to investigate how different controllers affect the behaviour of the vehicle, which is important due increased need for simulations and analysis in the early stages of a development process. Hence, the primary contribution of this project is a study that comprises design and implementation of active and semi-active cab suspensions in an Adams model of a complete vehicle, with the aim to improve ride comfort.

1.2 Purpose

The main purpose of this project is to design and implement active and semi-active cab suspensions in complete vehicle models with the goal to improve ride comfort. The focus of the study is the vertical dampers that are part of both the front and the rear cab suspensions. Handling features are also studied to ensure at least equivalent performance when substituting the conventional cab suspension system. A major part of this project aims to develop a method to implement control systems in Adams/Car, which is a software used by Volvo GTT today for vehicle design and simulation.

To achieve the goal of the thesis project, intermediate targets are defined and the study is carried out by taking the following steps:

- Define comfort and handling and determine how they are measured and quantified.
- Define load cases to evaluate the performance of the cab suspensions
- Perform benchmark tests with the conventional suspensions
- Design and implement active and semi-active controllers in Adams/Car
- Perform vehicle analysis with active and semi-active cab suspensions
- Evaluate the results in terms of comfort and handling

1.3 Limitations

For the execution of the thesis project to be feasible and to be able to deliver within the time frame, the scope of the project is based on the following limitations:

- The geometry of the vehicle and the pivot points of the suspension are unchanged
- The performance of the suspensions is evaluated from the following load cases and manoeuvres: driving on a rough road, driving on a smooth road, performing a single lane change and driving through a long dip.
- The vehicle is assumed to be fully loaded
- Roll, pitch and yaw rotation of the driver will not be considered
- Aerodynamic forces will not be considered
- The engine will not be considered as a vibration source

1.4 Report outline

The structure of the report is designed in order to present the work flow in a transparent and orderly manner. A brief description of the outline is presented here to help orient the reader in the project report.

The report starts with a theory chapter, which presents and describes the truck models, the terms comfort and handling and the different control strategies and control algorithms upon which this project is based. The classical method chapter is here divided into two separate chapters, where the first part comprise benchmark tests for comparison and the second part describes controller design and implementation as well as the analysis that were performed. In the following chapter are the results from the analysis presented and evaluated. Thereafter follows a compilation and discussion of the results as well as recommendations for future work. The report is completed with a presentation of the conclusions of the thesis project.

2 Theory

This chapter provides information and descriptions of some basic terms and theories that are needed for the project. The chapter also includes explanations of the assumptions and simplifications that were done during the execution of the project. The scope of the chapter is written with a reader with a background from mechanical engineering in mind.

2.1 The truck

The truck model that is studied in this thesis is a Volvo FH tractor, for which a semitrailer can be connected through a clutch called the fifth wheel, see figure 2.1. The opposite variant is simply called trucks, or rigids, which indicates that the trailer is placed onto a rigid frame. However, to avoid confusion the studied vehicle (tractor semi-trailer combination) will be referred to as a truck throughout the report. The maximum gross combination weight is 42 ton.

General when describing a truck is that the Cartesian coordinate system is placed such that the positive direction of the x-axis goes from the front of the truck to rear in the longitudinal direction, the y-axis is in the lateral direction and z-axis in the vertical direction, see Figure 2.1. From this is cab roll defined as rotation about the longitudinal axis, cab pitch is rotation about the lateral axis and heave is the vertical motion of the cab, see Figure 2.2

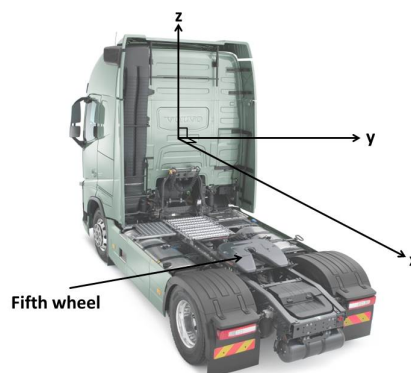


Figure 2.1: *Coordinate system for the truck*

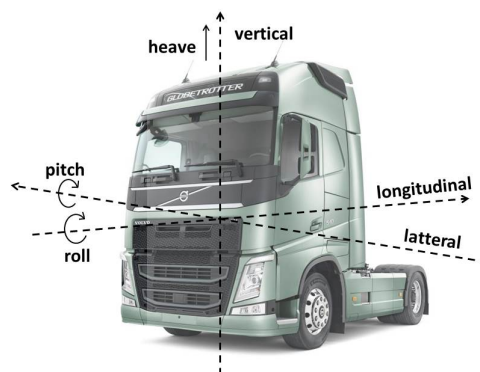


Figure 2.2: *Cab pitch, roll and heave*

2.1.1 Cab suspension

The cab is supported via the chassis by suspensions in the front and rear of the cab. The front suspensions consist of bushings that absorb forces in the vertical, lateral and longitudinal direction and spring-dampers that take up forces in the vertical direction. In the rear, there are spring-damper combinations in the vertical direction and dampers that absorb forces in the lateral direction. It is mainly the vertical dampers that affect the ride comfort when the truck is operated on a flat road with road vibration input. With the primary objective to improve the ride comfort, it was chosen to focus this study on the vertical dampers, which are substituted with active and semi-active dampers in the analysis.

To protect the suspensions when the cab is experiencing large relative motions, there are bump and rebound stops in the front and in the rear of the cab. The rubber stops also aid to avoid hard impact between the cab and the chassis. The front bump and rebound stop consists of a two rubber blocks that are separated with a metal plate. The upper and lower rubber blocks correspond to the rebound stop and bump stop respectively and have different characteristics. The rubber blocks are connected to the cab through a stiff wire that runs to through an opening in chassis. A schematic sketch is shown in Figure 2.3. Both the upper and lower walls are part of the chassis. When the cab moves upwards relative to the chassis, the rebound stop will eventually engage and prevent the on-going motion. Similarly, when the relative motion between the cab and the chassis is negative, the bump stop will eventually reach the lower wall, preventing the cab and the chassis to come into contact. In the rear is the bump stop and rebound stop integrated in the damper but which works in a similar way with rubber blocks that controls the relative motion between the cab and the chassis.

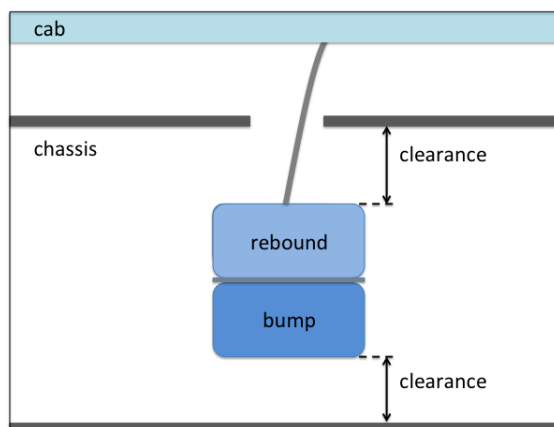


Figure 2.3: Schematic sketch of the bump stop and rebound stop in the front cab suspensions

The characteristics of each rubber block are represented by a force-displacement curve, which determines the maximum force and the pertinent displacement of the rubber block once they are engaged. The distance the rubber blocks can move before reaching the upper and lower walls is defined by the clearance in the different directions.

2.1.2 Truck model

The models of the trucks are developed in Adams/Car and are provided by Volvo GTT. Two main models are available; one complete model of the tractor semi-trailer combination and one model of the tractor only, for which the trailer is represented as a point mass acting on fifth wheel. General for both models are the frame and the stabilizer bars, one in the front and one in the rear, are modelled as flexible parts and the cab and the semitrailer are modelled as rigid parts. The structure of the cab has an uneven weight distribution due to e.g. the position of driver, seat and steering wheel, which cause the centre of gravity to have a small offset from the x-axis.

The complete assemblies consists of several subsystems, e.g. cab, frame, wheels and brake system, which all are constructed individually. The cab suspension is included in the cab subsystem. The springs and dampers are modelled using force elements between the installation points and are described with force-displacement and force-velocity curves respectively. The springs are modelled as linear air springs while the damping properties are non-linear. The springs are also defined with a length and a preload that correspond to the static solution of the real vehicle. All springs are defined with the same preload, which results in a small roll angle of the cab after solving the static equilibrium due to the unsymmetrical weight distribution of the cab.

Tyre-model

The primary task of the tyres is to provide tyre grip and traction for the truck. The task is also to transfer forces and to isolate the vehicle from vertical disturbances. The tyres should roll with minimal energy loss and cause minimal emissions of particles and noise. The properties of the tyres greatly influence the dynamical behaviour of the vehicle since the most of the interactions with the environment are transferred through the tyres. When the vehicle is travelling and the tyres roll over a flat, smooth surface, many complex phenomena occurs. These phenomena are e.g. deformation of the tyres that cause varying radii and longitudinal and lateral wheel slip that induce frictional forces [8].

Two different tyre-models called PAC2002 and FTire are used in the simulations, which both are included in the MSC software [9]. The PAC2002-tyre is a Magic-Formula (MF) tyre model developed according to Tyre and Vehicle Dynamics by Pacejka [10]. Magic-Formula is one of the most well-known curve fit models which uses trigonometric functions to curve fit experimental data [8].

In general, a MF tyre model describes the behaviour of the tyre for rather smooth roads up to frequencies of 8 Hz. Thus, PAC2002-tyre models are mainly applicable for handling and stability simulations, which are evaluated for rather low frequencies [9].

The FTire model is developed by Cosin and is a complete tyre model that is designed for e.g. comfort simulations. The FTire is computationally more expensive then the PAC2002-tyre. It is fully non-linear and valid in frequency domain up to 120 Hz [11].

2.2 Comfort

The meaning of ride comfort is the comfort the driver experience from vibrations when the vehicle is traveling in a certain speed over a road that give rise to a certain excitation of the vehicle [8]. Comfort is a subjective measure but is evaluated according to Volvo GTT guidelines concerning ride comfort and vibrations [12]. These guidelines are based on the how the human body respond to vibrations in different directions according to ISO-2631 [13], where the RMS values of accelerations in different directions are filtered depending on human sensitivity. How this filter function works is further explained in Section 2.2.2. Ride comfort is mainly affected by frequencies in the range up to 20 Hz [7].

2.2.1 Ride comfort analysis

The ride comfort is analysed in Adams/Car using a road simulator, simulating a four-post rig test as illustrated in Figure 2.4. In a four-post rig test are the wheels of the truck placed on top of four actuators that can move individually. The movement of the actuators are controlled by digital input signals that simulate the surface of a road. The simulations in Adams/Car are executed in the same way, using virtual roads to control the movements of the actuators. The virtual roads are vibration noise, created to represent road surfaces pertinent to different road qualities.

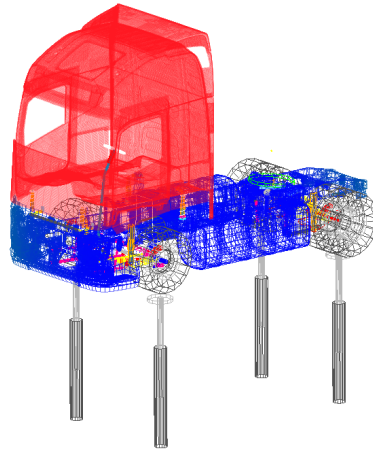


Figure 2.4: *Model of the tractor in a four-post test rig in Adams/Car for full-vehicle analysis*

The comfort analysis for a random road excitation is performed for driving velocity 70 km/h and with maximum load according to Volvo GTT guidelines. The accelerations are evaluated at two different positions in the cab, which are listed below.

- B-pillar on left hand side in longitudinal, lateral and vertical direction

- Cab front floor on right hand side in lateral direction

The position of the b-pillar is located in the cab structure, close to drivers left ear. The ISO-filtered RMS values at the position of the b-pillar are used to compute an overall comfort value, called a 3D value, which are used for evaluation and comparison, see Section 2.2.2.

Virtual roads

Volvo GTT defines road quality using four main categories; well maintained, less maintained, badly maintained and very badly maintained. A virtual road represents vibrations that correspond to a road surface with a certain road severity and is composed of distance and elevation data. The virtual roads can also include potholes that occur with varying frequency and depth to provide different road severities. In this thesis are two different road quality levels used in the analysis; less maintained and badly maintained. Neither of these roads includes transients. The less maintained road is composed of low road vibration and the badly maintained road corresponds to high road vibration. [14].

2.2.2 Vibrations and the human body

The human body is sensitive to vibrations. The human sensitivity is different depending on the frequency and the direction of the vibrations. By using a human filter function, the vibrations can be translated from vibration in space to how they are experienced inside the driver's brain, where discomfort is perceived. The human filter function is proposed in ISO-2631 and divides the sensitivity into two directions, horizontal and vertical [13]. The horizontal sensitivity function is used for both lateral and longitudinal accelerations. Table 2.1 shows how different RMS acceleration levels will be experienced by the driver [13].

| Acceleration magnitude [m/s ²] | Experience |
|--|-------------------------|
| Less than 0.315 | not uncomfortable |
| 0.315 to 0.63 | a little uncomfortable |
| 0,5 to 1 | fairly uncomfortable |
| 0.8 to 1.6 | uncomfortable |
| 1.25 to 2.5 | very uncomfortable |
| Greater than 2 | extremely uncomfortable |

Table 2.1: Human sensitivity to acceleration magnitudes

In ISO-2631, the human filter is presented as a transfer function with different sensitivities for different frequencies. In a vibrating system with only one frequency can the experienced discomfort easily be calculated by multiplying the acceleration magnitude with the corresponding sensitivity for that frequency. In real life, the vibrations are more complex and it's not possible to describe the signal using one frequency and one amplitude. By using Fourier transform, the signal can be transformed to a series of trigonometric functions in the frequency domain. These trigonometric functions can be filtered individually for each frequency and amplitude and then transformed back to the time domain where an RMS value can be calculated. The Fourier transform is calculated in Matlab using the discrete output acceleration data from Adams/Car using the Matlab function `fft`.

Human sensitivity transfer function

The human sensitivity transfer function is created by a combination of four transfer functions combining a low pass filter, a high pass filter, an acceleration-velocity transition filter and an upward step filter. All filters are of second order and the total filter is calculated using equation 2.1. For this case the complex variable, s , is equal to $j\omega$.

$$W_{tot}(s) = W_{HP}W_{LP}W_{AVT}W_{US} \quad (2.1)$$

The components in transfer function for accelerations in the horizontal plane is defined by equations 2.2-2.9.

$$f_1 = 0.4 \text{ Hz} \quad \omega_1 = 2\pi f_1 \text{ rad/s} \quad (2.2)$$

$$W_{d,HP} = \frac{s^2}{s^2 + \sqrt{2}\omega_1 s + \omega_1^2} \quad (2.3)$$

$$f_2 = 100 \text{ Hz} \quad \omega_2 = 2\pi f_2 \text{ rad/s} \quad (2.4)$$

$$W_{d,LP} = \frac{1}{1 + \frac{\sqrt{2}s}{\omega_2} + \frac{s^2}{\omega_2^2}} \quad (2.5)$$

$$f_3 = 2 \text{ Hz} \quad f_4 = 2 \text{ Hz} \quad q_4 = 0.63 \quad (2.6)$$

$$\omega_3 = 2\pi f_3 \text{ rad/s} \quad \omega_4 = 2\pi f_4 \text{ rad/s} \quad (2.7)$$

$$W_{d,AVT} = \frac{1 + s/\omega_3}{1 + \frac{s}{q_4\omega_4} + \frac{s^2}{\omega_4^2}} \quad (2.8)$$

$$W_{d,US} = 1 \quad (2.9)$$

The components in transfer function for acceleration in the vertical direction is defined by equations 2.10-2.19.

$$f_1 = 0.4 \text{ Hz} \quad \omega_1 = 2\pi f_1 \text{ rad/s} \quad (2.10)$$

$$W_{k,HP} = \frac{s^2}{s^2 + \sqrt{2}\omega_1 s + \omega_1^2} \quad (2.11)$$

$$f_2 = 100 \text{ Hz} \quad \omega_2 = 2\pi f_2 \text{ rad/s} \quad (2.12)$$

$$W_{k,LP} = \frac{1}{1 + \frac{\sqrt{2}s}{\omega_2} + \frac{s^2}{\omega_2^2}} \quad (2.13)$$

$$f_3 = 12.5 \text{ Hz} \quad f_4 = 12.5 \text{ Hz} \quad q_4 = 0.63 \quad (2.14)$$

$$\omega_3 = 2\pi f_3 \text{ rad/s} \quad \omega_4 = 2\pi f_4 \text{ rad/s} \quad (2.15)$$

$$W_{k,AVT} = \frac{1 + s/\omega_3}{1 + \frac{s}{q_4\omega_4} + \frac{s^2}{\omega_4^2}} \quad (2.16)$$

$$f_5 = 2.37 \text{ Hz} \quad f_6 = 3.35 \text{ Hz} \quad q_5 = 0.91 \quad q_6 = 0.91 \quad (2.17)$$

$$\omega_5 = 2\pi f_5 \text{ rad/s} \quad \omega_6 = 2\pi f_6 \text{ rad/s} \quad (2.18)$$

$$W_{k,US} = \frac{1 + \frac{s}{q_5\omega_5} + \frac{s^2}{\omega_5^2}}{1 + \frac{s}{q_6\omega_6} + \frac{s^2}{\omega_6^2}} \quad (2.19)$$

The shape of the two transfer functions can be seen in Figure 2.5.

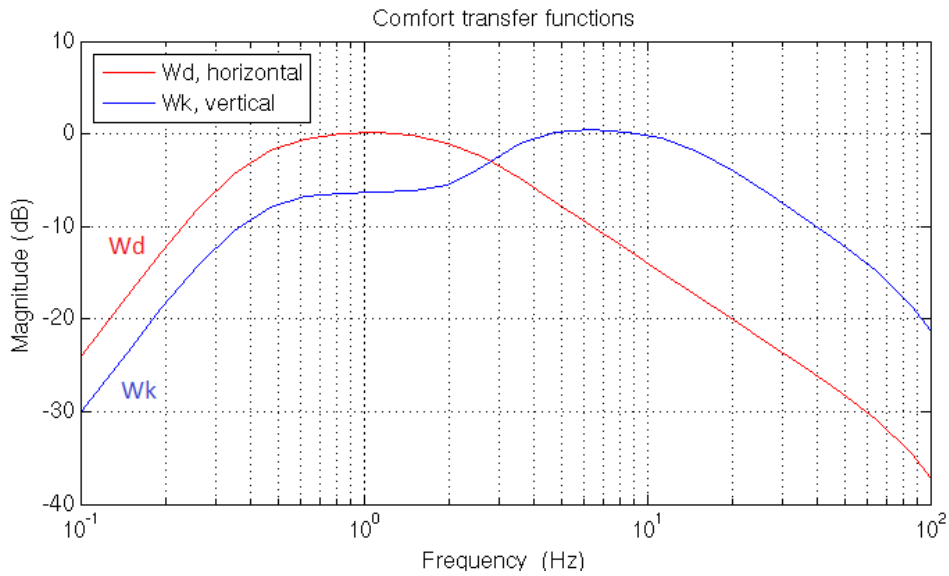


Figure 2.5: Sensitivity functions for horizontal and vertical accelerations

Vibrational 3D value

To measure the total vibration experience, the vibrations in all three dimensions needs to be combined. This is done by transforming the human sensitivity filtered accelerations in the frequency domain back to the time domain. To quantify the vibrations, the RMS value of the filtered acceleration data is calculated. The combined vibration data for all three dimension is called vibrational 3D value, or comfort value, and is according to ISO 2631[13] calculated using equation 2.20.

$$a_v = \sqrt{k_x^2 a_{rms,wx}^2 + k_y^2 a_{rms,wy}^2 + k_z^2 a_{rms,wz}^2} \quad (2.20)$$

Where k_i are factors that represent different load cases depending on if the person is standing, seated etc. When measuring comfort for seated persons, this factor is equal to 1 for all directions. $a_{rms,wi}$ is the RMS value of the weighted acceleration data in the longitudinal, lateral and vertical direction. A high 3D value corresponds to large vibrations and consequently, the lower 3D value, the better ride comfort.

2.3 Handling

Handling represents how the vehicle responds to driver steering, acceleration and braking. The objective is in general to achieve minimal time delay between driver input and vehicle response. Furthermore, the responses of the vehicle should be predictable and hence, strong non-linearities are undesired [15]. Handling is affected by frequencies that are lower compared to comfort and the range is usually between 2 – 4 Hz. The main factors that affect handling are vehicle properties such as mass, inertia, load distribution, steering characteristics, suspensions settings and tyre properties [16].

Similar to ride comfort, handling is a subjective measure that is expected to differ from driver to driver. When accelerating and braking in a commercial truck, cab heave and pitch motions become evident. The ideal response depends on how quickly the driver understands what is happening. When the accelerations are sufficiently evident for the driver to comprehend the situation, all heave and pitch motions can be fully suppressed. [15]

Both handling and safety issues are affected by the suspension design. For heavy vehicles are roll over tendencies one of the main important safety issues. However, damping characteristics have small influence on roll over, which is highly affected by the height of the centre of mass and spring stiffness. Damper tuning has in turn great influence on handling manoeuvres, such as a single lane change that are a dynamic event. Position and setting of the damper effect the normal tyre force variation and dynamic load distribution in a large extent [16].

2.3.1 Handling analysis

Vehicle handling is currently evaluated from different manoeuvring tests from both real world handling and from finite element simulations at Volvo GTT. Standard simulations for complete vehicle handling analysis are steady state and random steering tests where handling is evaluated based on e.g. the global cab roll angle and the total understeer gradient. The handling analysis differs from comfort simulations in that sense that the vehicle travels over a smooth road, using a road model instead of the road simulator. The truck model used in the handling analysis is the complete truck and semitrailer combination. Since the focus of this thesis is to study the cab suspensions, and in particular the damper properties, it is relevant to study a dynamic event [16]. It was therefore chosen to evaluate vehicle handling and the performance of the suspension based on single lane change and from the attitudes listed below.

- Cab roll angle (Global)
- Cab roll angle (Relative chassis)
- Cab pitch angle
- Lateral acceleration in central of gravity (cab)
- Lateral acceleration in front axle

In general, it is desired to have small rotations around the horizontal axes and small lateral accelerations in the cab and front axle as well as minimized delay from the steering wheel input. Figure 2.6 shows how the global roll angle and the relative roll angle are defined. The figure is a schematic sketch of the cab, chassis and wheels and how they are connected through suspensions, looking in the longitudinal direction.

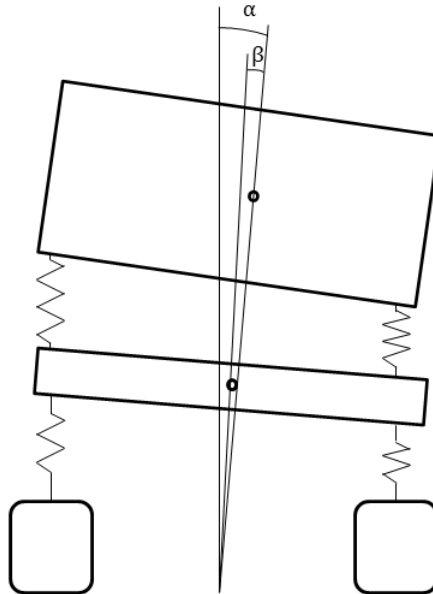


Figure 2.6: Global roll angle α and relative roll angle β

2.4 Cab model

The cab is modelled as a rigid body with three degrees of freedom; heave (z), roll (θ_x) and pitch (θ_y), see Figure 2.7. The majority of the motions of the cab can be described through the heave, roll and pitch motions, which is the reason why the cab is modelled using these particular degrees of freedom. The cab is modelled with four suspension points, two in the front and two in the rear. The variables have an index where the first letter denotes front or rear, f/r , and the second letter denotes left or right, l/r . Each suspension point is connected to a spring and a damper in parallel with an force actuator. The springs and the dampers are modelled using linear elements. The actuator forces are denoted by F_{ij} and are supplied by the control system. The displacements of the upper suspension points are denoted z_{ij} and the displacements of the lower suspension points in the chassis are denoted u_{ij} . The parameters pertinent to the cab model are shown in Table 2.2.

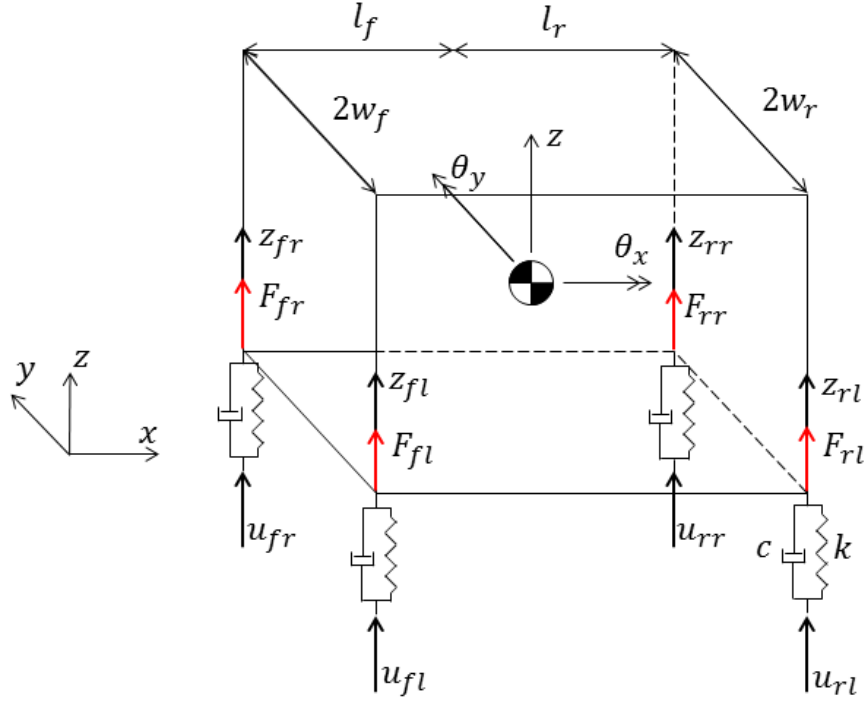


Figure 2.7: Three degree of freedom cab model

| | |
|--|------------|
| Cab mass | m |
| Pitch moment of inertia | J_x |
| Roll moment of inertia | J_y |
| Suspension spring stiffness | k |
| Suspension damping coefficient | c |
| Distance between the c.o.g. and the upper suspension points along the y-axis | w_f, w_r |
| Distance between the c.o.g. and the upper suspension points along the x-axis | l_f, l_r |

Table 2.2: Notations for parameters used to describe the three-degree of freedom cab model.

The positions of the upper suspension points are given by the kinematic relations in equation 2.21.

$$\begin{bmatrix} z_{fl} \\ z_{fr} \\ z_{rl} \\ z_{rr} \end{bmatrix} = \begin{bmatrix} 1 & -w_f & l_f \\ 1 & w_f & l_f \\ 1 & -w_r & -l_r \\ 1 & w_r & -l_r \end{bmatrix} \begin{bmatrix} z \\ \theta_x \\ \theta_y \end{bmatrix} \quad (2.21)$$

The forces exerted by the suspension system in each corner are denoted by $F_{ij,tot}$. The equations of motion of the cab can be written in the following way.

$$m\ddot{z} = F_{fl,tot} + F_{fr,tot} + F_{rl,tot} + F_{rr,tot} \quad (2.22)$$

$$J_x\ddot{\theta}_x = -F_{fl,tot}w_f + F_{fr,tot}w_f - F_{rl,tot}w_r + F_{rr,tot}w_r \quad (2.23)$$

$$J_y\ddot{\theta}_y = F_{fl,tot}l_f + F_{fr,tot}l_f - F_{rl,tot}l_r - F_{rr,tot}l_r \quad (2.24)$$

The force in each suspension point can be calculated as

$$F_{ij,tot} = -k(z_{ij} - u_{ij}) - c(\dot{z}_{ij} - \dot{u}_{ij}) + F_{ij} \quad (2.25)$$

Where k is the spring coefficient, c is the damping coefficient, z_{ij} is the position of the upper suspension points, u_{ij} is the lower suspensions points and F_{ij} is the force applied by the actuator. F_{ij} is equal to zero if the system is passive. When an active or a semi-active control system is connected, c is set to 0 instead.

Instead of writing the equations of motion as a function of the coordinates of the suspension system, it is possible to write them as a function of the modal coordinates, the heave, roll and pitch motions. This is done by using equation 2.21. This transformation makes it possible to express the motion of the cab in its own coordinate system, which is used to write the system in state space form. The state space form is formulated in the following way

$$\dot{\mathbf{x}} = \mathbf{A}\mathbf{x} + \mathbf{B}\mathbf{u} \quad (2.26)$$

$$\mathbf{y} = \mathbf{C}\mathbf{x} + \mathbf{D}\mathbf{u} \quad (2.27)$$

$$\mathbf{A} = \mathbf{M}^{-1} \begin{bmatrix} 0 & 0 & 0 & 1 & 0 & 0 \\ 0 & 0 & 0 & 0 & 1 & 0 \\ 0 & 0 & 0 & 0 & 0 & 1 \\ -4k & 0 & -2k(l_f - l_r) & -4c & 0 & -2c(l_f - l_r) \\ 0 & -2k(w_f^2 + w_r^2) & 0 & 0 & -2c(w_f^2 + w_r^2) & 0 \\ -2k(l_f - l_r) & 0 & -2k(l_f^2 + l_r^2) & -2c(l_f^2 - l_r^2) & 0 & -2c(l_f^2 + l_r^2) \end{bmatrix} \quad (2.28)$$

$$\mathbf{B} = \mathbf{M}^{-1} \begin{bmatrix} 0 & 0 & 0 & 0 & 0 & 0 & 0 & 0 & 0 & 0 & 0 & 0 \\ 0 & 0 & 0 & 0 & 0 & 0 & 0 & 0 & 0 & 0 & 0 & 0 \\ 0 & 0 & 0 & 0 & 0 & 0 & 0 & 0 & 0 & 0 & 0 & 0 \\ k & k & k & k & c & c & c & c & 1 & 1 & 1 & 1 \\ -kw_l & kw_r & -kw_l & kw_r & -cw_l & cw_r & -cw_l & cw_r & -w_l & w_r & -w_l & w_r \\ kl_f & kl_f & -kl_r & -kl_r & cl_f & cl_f & -cl_r & -cl_r & l_f & l_f & -l_r & -l_r \end{bmatrix} \quad (2.29)$$

$$\mathbf{C} = \mathbf{I}, \mathbf{D} = \mathbf{0} \quad (2.30)$$

Where \mathbf{x} contains the state variables of the system and $\dot{\mathbf{x}}$ is its time derivatives. \mathbf{u} is the system input and consists of the position and velocity of the chassis and the actuator forces. \mathbf{M} is the mass matrix of the system. \mathbf{M} , \mathbf{x} and \mathbf{u} and are defined as

$$\mathbf{M} = \begin{bmatrix} 1 & 0 & 0 & 0 & 0 & 0 \\ 0 & 1 & 0 & 0 & 0 & 0 \\ 0 & 0 & 1 & 0 & 0 & 0 \\ 0 & 0 & 0 & m & 0 & 0 \\ 0 & 0 & 0 & 0 & J_x & 0 \\ 0 & 0 & 0 & 0 & 0 & J_y \end{bmatrix} \quad (2.31)$$

$$\mathbf{x} = [z \quad \theta_x \quad \theta_y \quad \dot{z} \quad \dot{\theta}_x \quad \dot{\theta}_y]^T \quad (2.32)$$

$$\mathbf{u} = [u_{fl} \quad u_{fr} \quad u_{rl} \quad u_{rr} \quad \dot{u}_{fl} \quad \dot{u}_{fr} \quad \dot{u}_{rl} \quad \dot{u}_{rr} \quad F_{fl} \quad F_{fr} \quad F_{rl} \quad F_{rr}]^T \quad (2.33)$$

This cab model has several simplifications compared to the model in Adams/Car. The following features are neglected:

- The stabilizer bar
- The rear lateral dampers
- The bushings
- The bump stops and rebound stops
- Longitudinal and lateral motion

This simplified model gives the possibility to run analyses in Matlab with a significantly shorter simulation time compared to Adams. Furthermore, Linear Quadratic Regulator (LRQ), which is introduced later in Section 2.6.3, is a control strategy, which is based on this state space model.

2.4.1 Estimating the modal coordinates

The modal coordinates are given by the heave, roll and pitch motions in the center of gravity of the cab. State variables are often denoted by the displacements and the velocities in terms of these coordinates, which are input to several control strategies that are introduced later in this chapter. The idea to base the control strategy on the modal coordinates, also called modal control, was introduced by Lotus [17]. Since it is not feasible to measure z , θ_x or θ_y in the center of gravity, these values are calculated from the positions and velocities of the upper suspension points, see equations 2.34-2.36. The velocities is obtained in a similar way, according to equations 2.37-2.39. Small angles can be assumed.

$$z = \frac{z_{fl} + z_{fr}}{2L}l_r + \frac{z_{rl} + z_{rr}}{2L}l_f \quad (2.34)$$

$$\theta_x = \frac{z_{fr} - z_{fl}}{2w_f L}l_r + \frac{z_{rr} - z_{rl}}{2w_r L}l_f \quad (2.35)$$

$$\theta_y = \frac{z_{fl} + z_{fr}}{2L} - \frac{z_{rl} + z_{rr}}{2L} \quad (2.36)$$

$$\dot{z} = \frac{\dot{z}_{fl} + \dot{z}_{fr}}{2L}l_r + \frac{\dot{z}_{rl} + \dot{z}_{rr}}{2L}l_f \quad (2.37)$$

$$\dot{\theta}_x = \frac{\dot{z}_{fr} - \dot{z}_{fl}}{2w_f L}l_r + \frac{\dot{z}_{rr} - \dot{z}_{rl}}{2w_r L}l_f \quad (2.38)$$

$$\dot{\theta}_y = \frac{\dot{z}_{fl} + \dot{z}_{fr}}{2L} - \frac{\dot{z}_{rl} + \dot{z}_{rr}}{2L} \quad (2.39)$$

2.4.2 Modal force distribution

One approach to control the motions of the cab is, as mentioned, to control damping of the modal coordinates. Several papers exist that investigate the modal approach on damping in passenger cars and e.g. Bae et al [18] presents damping control with semi-active dampers that combine the skyhook theory with the modal approach on damping.

The modal coordinates are used in the control algorithm to determine the desired forces and torques in the centre of gravity of the cab, denoted by F_{heave} , M_{roll} and M_{pitch} . These forces and torques needs to be translated into control forces, F_{fl} , F_{fr} , F_{rl} and F_{rr} , that can be applied through the actuators. The relations between the desired forces and torques and the actuator forces are seen in equations 2.40-2.42.

$$F_{heave} = F_{fl} + F_{fr} + F_{rl} + F_{rr} \quad (2.40)$$

$$M_{roll} = -F_{fl}w_f + F_{fr}w_f - F_{rl}w_r + F_{rr}w_r \quad (2.41)$$

$$M_{pitch} = F_{fl}l_f + F_{fr}l_f - F_{rl}l_r - F_{rr}l_r \quad (2.42)$$

This system of equations has four unknown forces but only three equations, which gives an infinite set of possible solutions. To make the system statically determined it is necessary to introduce an extra linearly independent equation so that the system becomes invertible. One way to add an extra equation is to add a restriction to how the forces are distributed. This is done by imposing a requirement on the warp torque applied by the control forces, saying that the warp should be zero. The warp motion can be described as twisting of the cab, which is an undesired motion. Warp is prevented by introducing the following equation:

$$F_{fl}w_f - F_{fr}w_f = F_{rl}w_r - F_{rr}w_r \quad (2.43)$$

Or equally

$$F_{fl}w_f - F_{fr}w_f - F_{rl}w_r + F_{rr}w_r = 0 \quad (2.44)$$

These four equations now form a system of equations that have a unique solution and that fulfils the equations 2.40-2.42.

$$\begin{bmatrix} 1 & 1 & 1 & 1 \\ -w_f & w_f & -w_r & w_r \\ l_f & l_f & -l_r & -l_r \\ w_f & -w_f & -w_r & w_r \end{bmatrix} \begin{bmatrix} F_{fl} \\ F_{fr} \\ F_{rl} \\ F_{rr} \end{bmatrix} = \begin{bmatrix} F_{heave} \\ M_{roll} \\ M_{pitch} \\ 0 \end{bmatrix} \quad (2.45)$$

2.5 Passive vibration control

The basics of passive vibration control are presented here to introduce important terminology and study some of the basic concepts. A passive control system can absorb structural vibrations and remove energy from the dynamic system without an external energy source. The technique is to link the structure to components and materials with damping properties that suppresses vibrations. A passive system is generally equipped with springs and dampers with time invariant stiffness and damping coefficients [2].

To study the dynamics, a single-degree-of-freedom system is considered. The system contains a mass, a linear spring and a linear damper. The system can be seen in Figure 2.8. m is the mass, k is the spring coefficient, c is the damper coefficient and x is the coordinate of the mass.

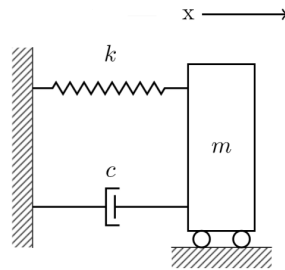


Figure 2.8: *Single-degree-of-freedom system*

The equation of motion for the system can be written as

$$m\ddot{x} + c\dot{x} + kx = F(t) \quad (2.46)$$

Assuming that the applied force $F(t) = 0$ gives that

$$m\ddot{x} + c\dot{x} + kx = 0 \quad (2.47)$$

The equation of motion can also be written on the following form

$$\ddot{x} + 2\zeta\omega_n\dot{x} + \omega_n^2x = 0 \quad (2.48)$$

Where $\omega_n = k/m$ and $\zeta = c/(2m\omega_n)$. The general solution of equation 2.48 can be written as

$$x(t) = A_1e^{\lambda_1t} + A_2e^{\lambda_2t} \quad (2.49)$$

A_1 and A_2 are determined by the initial conditions of the system and λ_1 and λ_2 are the roots of the following equation

$$\lambda^2 + 2\zeta\omega_n\lambda + \omega_n^2 = 0 \quad (2.50)$$

The roots λ_1 and λ_2 are calculated by solving the following equation

$$\lambda_1 = \omega_n \left(-\zeta + \sqrt{\zeta^2 - 1} \right), \lambda_2 = \omega_n \left(-\zeta - \sqrt{\zeta^2 - 1} \right) \quad (2.51)$$

2.5.1 Undamped system

The case where $\zeta = 0$ is called an undamped system and has the following solution

$$x(t) = a_1 \cos \omega_n t + a_2 \sin \omega_n t \quad (2.52)$$

The constants a_1 and a_2 are determined by the initial conditions of the system. Since there is no damping, the system will continue oscillate with the same frequency and amplitude.

2.5.2 Underdamped system

In the case where $0 < \zeta < 1$ can the general solution be written as

$$x(t) = e^{-\zeta\omega_n t} (A_1 e^{i\sqrt{1-\zeta^2}\omega_n t} + A_2 e^{-i\sqrt{1-\zeta^2}\omega_n t}) \quad (2.53)$$

Using the relation that $e^{i\omega t} = \cos \omega t + i \sin \omega t$, equation 2.53 can be rewritten as

$$x(t) = A e^{-\zeta\omega_n t} \cos(\omega_n \sqrt{1-\zeta^2} t - \varphi) \quad (2.54)$$

The mass will have an oscillating motion but it's amplitude will decrease over time. The case is called an underdamped system because of it's oscillating motion.

2.5.3 Critically damped system

A special case is when $\zeta = 1$. This makes $\lambda_1 = \lambda_2$ according to equation 2.51. In that case, the solution of the differential equation can be written as

$$x(t) = (A_1 + tA_2)e^{-\omega_n t} \quad (2.55)$$

This case is called critical damping since it's the fastest converging system without an any oscillating behavior.

2.5.4 Overdamped system

The last case is when $\zeta > 1$. The solution of the differential equation can then be written as

$$x(t) = e^{-\zeta\omega_n t} (A_1 e^{\omega_n t \sqrt{\zeta^2 - 1}} + A_2 e^{-\omega_n t \sqrt{\zeta^2 - 1}}) \quad (2.56)$$

This case is slower than the critically damped and is therefore called an overdamped system.

2.5.5 Characteristic response

The step response for the different cases can be seen in Figure 2.9, which shows the characteristic response for different ζ . The initial condition is $x(0) = 1, \dot{x}(0) = 0$.

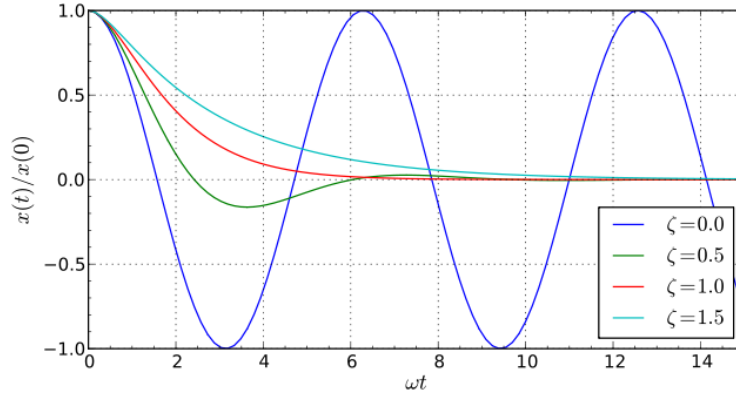


Figure 2.9: Step response for different values of ζ

2.6 Active vibration control

A system using active vibration control has the possibility to add and remove energy from the system through the use of actuators that apply forces or torques to the structure. The system can through the use of electric or hydraulic actuators generate forces independent of the state of the system. Consequently, an external energy source is needed, which results in that active systems are larger, more energy consuming and more expensive than both passive and semi-active control systems. In addition to increased complexity of the system, another drawback is the stability of the system in case of system failure, e.g. defective sensors [4]. The advantage is that they are more powerful and generally provides better performance. [19].

Two different strategies using skyhook theory are evaluated in the project, which is referred to as individual control and modal control. The concept with individual control is to control each damper individually. That is, the damping force mainly depend on the state of the suspension itself and is independent if the other dampers and the overall motion of the cab. Advantages with this approach are that it is simple to implement and easy to overview. Modal skyhook is a combination of the skyhook theory and the modal approach on damping, described in Section 2.4.1. The objective with modal skyhook is to consider the complete motion of the cab and and the main difference from individual control is that the damping forces are based on the modal coordinates, i.e. heave, roll and pitch. The active control laws that are studied in this thesis are presented below.

Individual Skyhook A simple control algorithm based on skyhook theory. The aim is to suppress the motion of every suspension point using active control.

Modal Skyhook A more advanced version of Individual Skyhook where the aim is to suppress the motion of the modal coordinates of the cab, using active control.

Linear Quadratic Regulator A control algorithms that use the solution of the Ricatti equation to find the optimal solution of a state space problem given the user defined penalty matrices.

2.6.1 Individual Skyhook

The concept of skyhook logic was initially proposed by Karnopp in 1974 [4]. In skyhook logic is the sprung mass imagined to be connected to a fixed point in the sky through a damper. The damping force can be written as

$$F_{sky} = c_{sky}\dot{x}_1(t) \quad (2.57)$$

Where \dot{x}_1 is the velocity of the sprung mass, i.e. the cab. Clearly, this is not feasible due to the need for mobility in vehicle applications. However, the concept of the skyhook control can be simulated by connecting the system to actuators that can add energy to the system regardless of the state of the system. In this case is the damping force applied between the sprung mass and another mass in the system, here between the cab and the chassis. In active control, for which the actuators can apply forces independent of the state of the system, the control algorithm simply becomes:

$$F_a = c_{sky}\dot{x}_1(t) \quad (2.58)$$

Where F_a is the active control force.

2.6.2 Modal Skyhook

In Modal skyhook, the aim is to control the modal motions represented by the heave, pitch and roll motions of the cab. The desired forces and torques acting on the cab are defined as

$$F_{heave} = -c_{heave}\dot{z} \quad (2.59)$$

$$M_{roll} = -c_{roll}\dot{\theta}_x \quad (2.60)$$

$$M_{pitch} = -c_{pitch}\dot{\theta}_y \quad (2.61)$$

Where, the state variables \dot{z} , $\dot{\theta}$ and $\dot{\theta}$, are calculated according to equations 2.37-2.39. The desired forces and torques are then translated to damping forces by solving equation 2.45.

2.6.3 Linear Quadratic Regulator

Linear quadratic regulator, LQR, is a control strategy with the objective to minimize the cost function

$$J = \frac{1}{2} \int_0^{\infty} (\mathbf{x}^T \mathbf{Q} \mathbf{x} + \mathbf{u}^T \mathbf{R} \mathbf{u}) dt \quad (2.62)$$

for a given linearized system on state space form

$$\dot{\mathbf{x}}(t) = \mathbf{A}\mathbf{x}(t) + \mathbf{B}\mathbf{u}(t) \quad (2.63)$$

Where \mathbf{A} is the state matrix and \mathbf{B} is the control matrix. $\mathbf{x} = [x_1, x_2, \dots, x_n]^T$ is the state vector of the system, and $\mathbf{u} = [u_1, u_2, \dots, u_m]^T$ is the vector containing the control input. The matrices \mathbf{Q} and \mathbf{R} are designed based on how the states and the forces should be weighted in the cost function. \mathbf{Q} is defined as a semi definite and

symmetric matrix and \mathbf{R} is a positive definite and symmetric matrix. A simple way to write these matrices is shown in equation 2.64

$$\mathbf{Q} = \begin{bmatrix} q_1 & 0 & \cdots & 0 \\ 0 & q_2 & \cdots & 0 \\ \vdots & \vdots & \ddots & \vdots \\ 0 & 0 & \cdots & q_n \end{bmatrix}, \quad \mathbf{R} = \begin{bmatrix} r_1 & 0 & \cdots & 0 \\ 0 & r_2 & \cdots & 0 \\ \vdots & \vdots & \ddots & \vdots \\ 0 & 0 & \cdots & r_m \end{bmatrix} \quad (2.64)$$

The integrand in the cost function can then be written as:

$$q_1 x_1^2 + q_2 x_2^2 + \dots + q_n x_n^2 + r_1 u_1^2 + r_2 u_2^2 + \dots + r_n u_n^2 \quad (2.65)$$

The weighting matrices \mathbf{Q} and \mathbf{R} are commonly found from an iterative process to assure that the control system meets the design goals. If, for example, it's important to keep the value of the variable x_1 small, the corresponding penalty q_1 should be high. In general, if the states should be kept small, the element in \mathbf{Q} should have large values. Furthermore, if the control parameter u_1 should be kept small, the corresponding value of r_1 should be high. On the other hand, if u_1 is allowed to be large, r_1 can be set to a small value. This is a simple but straightforward approach to help define the \mathbf{Q} and \mathbf{R} depending on the priority of the state variables.

The optimal control law \mathbf{u}_* , which minimizes the objective function in equation 2.62 is given by

$$\mathbf{u}_* = -\mathbf{G}\mathbf{x}(t) \quad (2.66)$$

\mathbf{G} is defined as the gain matrix and is calculated from the following equation:

$$\mathbf{G} = \mathbf{R}^{-1}\mathbf{B}^T\mathbf{S} \quad (2.67)$$

In this equation is \mathbf{R} known and \mathbf{B} comes from the state space model. \mathbf{S} is called the Riccati matrix and is the solution of the algebraic nonlinear Riccati matrix equation.

$$\mathbf{A}^T\mathbf{S} + \mathbf{S}\mathbf{A} - \mathbf{S}\mathbf{B}\mathbf{R}^{-1}\mathbf{B}^T\mathbf{S} + \mathbf{Q} = \mathbf{0} \quad (2.68)$$

Solving the Riccati equation for a given \mathbf{Q} and \mathbf{R} will give the optimal control. The closed-loop system can then be written as

$$\dot{\mathbf{x}} = (\mathbf{A} - \mathbf{B}\mathbf{G})\mathbf{x} \quad (2.69)$$

Here, the LQR state space model is based on the cab model described in Section 2.4, but with further simplifications to make it implementable. The movement of the chassis is neglected and thus, it is assumed that the cab suspensions are connected to ground. Furthermore, the dampers are removed, which is done by setting the damping coefficient $c = 0$. These simplifications results in new \mathbf{A} and \mathbf{B} matrices. Removing the dampers gives a new \mathbf{A} -matrix, see equation 2.70. Since LQR is defined in a way such that \mathbf{u} now only contains the control forces, it is also necessary to update the \mathbf{B} -matrix. The elements corresponding to the lower positions and velocity of the suspensions are removed so that \mathbf{B} only contains information pertinent to the control forces. The LQR adapted \mathbf{B} -matrix is seen in equation 2.71.

$$\mathbf{A} = \mathbf{M}^{-1} \begin{bmatrix} 0 & 0 & 0 & 1 & 0 & 0 \\ 0 & 0 & 0 & 0 & 1 & 0 \\ 0 & 0 & 0 & 0 & 0 & 1 \\ -4k & 0 & -2k(l_f - l_r) & 0 & 0 & 0 \\ 0 & -2k(w_f^2 + w_r^2) & 0 & 0 & 0 & 0 \\ -2k(l_f - l_r) & 0 & -2k(l_f^2 + l_r^2) & 0 & 0 & 0 \end{bmatrix} \quad (2.70)$$

$$\mathbf{B} = \mathbf{M}^{-1} \begin{bmatrix} 0 & 0 & 0 & 0 \\ 0 & 0 & 0 & 0 \\ 0 & 0 & 0 & 0 \\ 1 & 1 & 1 & 1 \\ -w_l & w_r & -w_l & w_r \\ l_f & l_f & -l_r & -l_r \end{bmatrix} \quad (2.71)$$

The state variables, \mathbf{x} , and the input to the system, \mathbf{u} , are given by:

$$\mathbf{x} = [z \quad \theta_x \quad \theta_y \quad \dot{z} \quad \dot{\theta}_x \quad \dot{\theta}_y]^T \quad (2.72)$$

$$\mathbf{u} = [F_{fl} \quad F_{fr} \quad F_{rl} \quad F_{rr}]^T \quad (2.73)$$

It is possible chose \mathbf{Q} and \mathbf{R} matrices that are not diagonal but since the motions in heave, roll and pitch are almost decoupled in the state space model it is chosen to use diagonal matrices.

With the known \mathbf{A} and \mathbf{B} matrices and for chosen \mathbf{Q} and \mathbf{R} it is possible to solve the Ricatti equation and obtain the corresponding gain matrix which gives the optimal control law \mathbf{u}_* from equation 2.66. Thus, the control forces are given by:

$$\mathbf{u}_* = [F_{fl} \quad F_{fr} \quad F_{rl} \quad F_{rr}]^T \quad (2.74)$$

2.7 Semi-active vibration control

Semi-active control systems can be described as a compromise between passive and active systems. It has the ability to change it's properties and thus, change the internal forces of the system in real-time but just as a passive system, it can only remove energy from the system. The idea was introduced already in 1974 by Karnopp [4]. Since no mechanical energy is added to the system, semi-active vibration control can be obtained with minimal energy consumption. The following two types of semi-active control systems are studied in this thesis, which both are based on skyhook theory.

Individual Skyhook A simple control algorithm based on skyhook theory. The aim is to suppress the motion of every suspension point using semi-active control.

Modal Skyhook A more advanced version of Individual Skyhook where the aim is to suppress the motion of the modal coordinates of the cab, using semi-active control.

2.7.1 Semi-active Individual Skyhook

The damping force using skyhook logic is again stated in equation 2.75.

$$F_{sky} = c_{sky}\dot{x}_1(t) \quad (2.75)$$

Different from active control, semi-active systems can only apply a force when the state of the system fulfils certain conditions. A semi-active damper can only generate force when the velocity of the cab, \dot{x}_1 , and the relative velocity over the suspension, $\dot{x}_1 - \dot{x}_2$, have the same sign. The state, when the semi-active damper can generate the desired force, is often referred to as "high state". When the cab and the relative velocity have opposite signs can the semi-active damper only provide a force in a opposite direction of the desired force. For optimal control, the damping force is then set to zero. This state is often referred to as "low state". Figure 2.10 illustrates how the system switch from high to low state depending on the velocity of the cab and the relative velocity over the suspension.

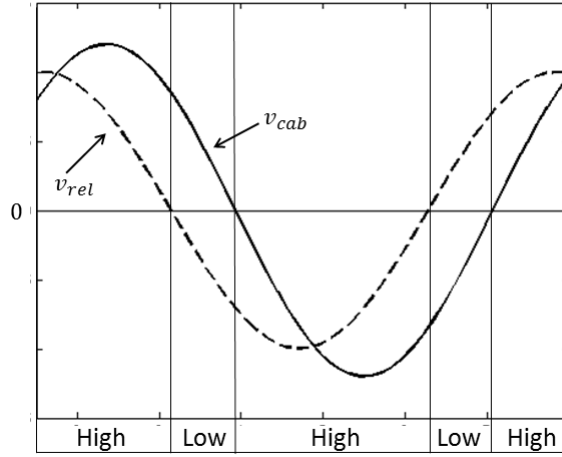


Figure 2.10: *Transition between high state and low state in semi-active control*

The control strategy can be described by equation 2.76. The strategy requires that the damping coefficient can be changed continuously and the control law is therefore known as continuous skyhook control.

$$F_{sa} = \begin{cases} c_{sky}\dot{x}_1, & \dot{x}_1(\dot{x}_1 - \dot{x}_2) \geq 0 \\ 0, & \dot{x}_1(\dot{x}_1 - \dot{x}_2) < 0 \end{cases} \quad (2.76)$$

In order to generate the desired damper force F_{sa} , the semi-active damper must fulfill the equation

$$F_{sa} = c_{sa}(\dot{x}_1 - \dot{x}_2) \quad (2.77)$$

By combining equation 2.76 and 2.77 the optimal damper coefficient for the damper can be calculated according to:

$$c_{sa} = \begin{cases} c_{sky} \frac{\dot{x}_1}{\dot{x}_1 - \dot{x}_2}, & \dot{x}_1(\dot{x}_1 - \dot{x}_2) \geq 0 \\ 0, & \dot{x}_1(\dot{x}_1 - \dot{x}_2) < 0 \end{cases} \quad (2.78)$$

2.7.2 Semi-active Modal Skyhook

The semi-active modal skyhook resembles the active modal control up to the stage when the forces and torques are distributed to the actuators. In addition, the same conditions as in the individual semi-active skyhook holds here, that is, the control system can only apply damping forces under certain conditions, i.e. when the system is in high state. Thus, the actuator force is controlled by the following equation.

$$F_{sa} = \begin{cases} F_{sa} & \dot{x}_1(\dot{x}_1 - \dot{x}_2) \geq 0 \\ 0, & \dot{x}_1(\dot{x}_1 - \dot{x}_2) < 0 \end{cases} \quad (2.79)$$

2.8 No-jerk Shape Function

A problem when using semi-active control algorithms is that a jerk can appear when changing from low state to high state, especially if there is a large peak in the damping force. It is easy to overlook this jerk when studying the acceleration curves obtained from simulations but which can be evident when riding in a vehicle

[7]. The discontinuities in the force can also cause numerical issues for the solver. A solution to this problem is to have a smooth transition between the states through the use of a shape function. A shape function, f , proposed by Ahmadian et al. [20] is given by equation 2.80.

$$f(v_{rel}) = 1 - e^{-\frac{|v_{rel}|}{v_0}} \quad (2.80)$$

The jerk-mitigated damping force, $F_{sa,nojerk}$, becomes:

$$F_{sa,nojerk} = F_{sa}f(v_{rel}) \quad (2.81)$$

In this equation, v_0 is a tuning variable that determines how fast the transition is. A low value gives a fast but jerky transition while a high value gives smooth but long transition. The value of v_0 must be optimized for best performance. For the minimum value, $v_0 = 0$ gives that $f \equiv 1$ while $v_0 = \infty$ gives $f \equiv 0$. The influence of the parameter v_0 is seen in Figure 2.11. It's important to be aware of that just before the relative velocity changes sign it is equal to zero and the shape function will therefore also be zero. When the relative velocity increases, the shape function will go towards 1. How fast depends on the value of v_0 .

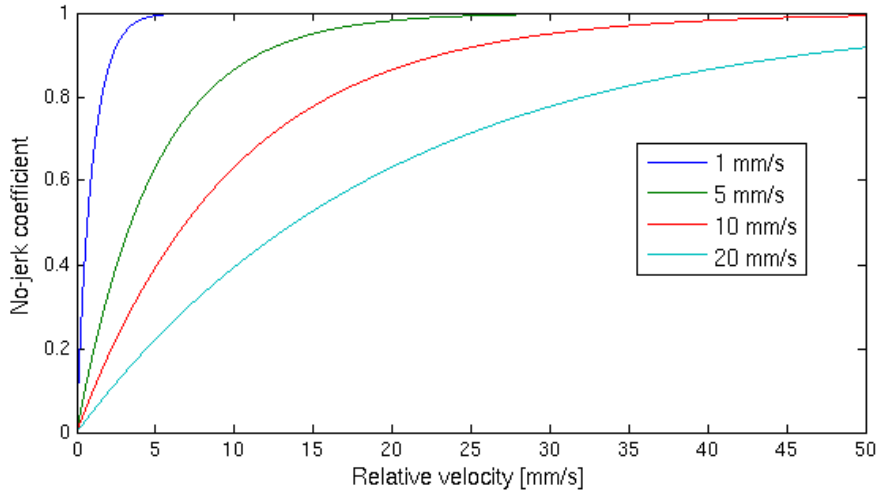


Figure 2.11: *No-jerk shape function*

A no-jerk block was built in simulink and can be seen in Figure 2.12. The gain in the gain block is equal to $1/v_0$. The block has the relative velocity, v_{rel} as input and the no-jerk factor, f , as the output.

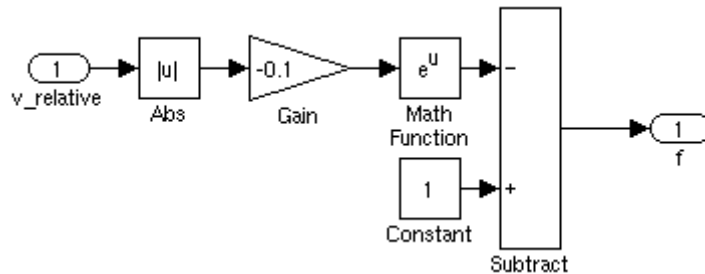


Figure 2.12: *The no-jerk module implemented in a simulink block*

3 Benchmark tests

To evaluate the conventional cab suspensions were different simulations carried out with the original passive dampers to create benchmark tests for comparison. Three different tests were designed with the purpose to evaluate the performance of the suspensions with respect to different vehicle feature. These tests are referred to as comfort, handling and long dip analysis. Initially, a sensitivity study was performed to study the influence of certain simulation parameters.

3.1 Sensitivity analysis

A sensitivity study was carried out by evaluating the response from a ride comfort analysis while changing selected parameters. The sensitivity analysis was conducted for the road quality level less maintained. The parameters that were assumed to influence the outcome were simulation time/driving distance, properties of the frame, tyre model, computational error and sampling frequency. The length of the virtual road is 1000 m, for which the driving velocity 70 km/h gives the maximum possible simulation time to be approximately 50 seconds before the road ends. The driving distance was thus varied by changing the time of the simulation, keeping constant speed. The chassis, or the frame, can either be flexible with partial coupling or rigid. The tyre models that were investigated were PAC2002 and FTire, see Section 2.1.2. The solver used for the simulations was the Adams/Car default solver, I3, for which the influence of the computational error was investigated. Below is a compilation of the result from the sensitive analysis, explaining the influence of the different parameters.

Frame The comfort value generally increases when switching from a rigid frame to a flexible frame. A flexible frame better captures the behaviour of the chassis compared to a rigid frame, presumably giving a more reliable response. A flexible frame is computationally more expensive than rigid frame.

Sampling frequency Sampling frequency was studied in the range between 100 – 500 Hz and the result shows increasing comfort values for increasing sampling frequency up to about 400 Hz. Above 400 Hz, the comfort value starts to converge.

Time Simulation time affects the comfort value but depends only on the current road profile that is included in the simulation.

Computational error The error was studied in the range between $1 \cdot 10^{-2}$ – $1 \cdot 10^{-4}$. The comfort value increases when the error decreases from $1 \cdot 10^{-2}$ to $1 \cdot 10^{-3}$ but the affect is small when further decreasing the error.

Tyre-model The comfort value generally increases when switching from the PAC2002 tyres to the FTire models, which can be explained by that road vibrations are better transferred though the FTire models. The simulation time increases with a factor of 3 – 4 with FTire compared to PAC2002.

The simulation setting was based on the findings from this sensitivity analysis. The sampling frequency was for all simulation set to 400 Hz, giving a Nyquist frequency of 200 Hz which is well above the range of interest. The properties of the frame clearly affect the output and it was chosen to use a flexible frame to capture the important eigen modes of the frame. The computational error was set to $1 \cdot 10^{-3}$. The other parameters were chosen depending on the analysis at hand. The simulation settings for the different kind of analysis and the benchmark tests are presented below.

3.2 Comfort

To evaluate ride comfort for different active and semi-active dampers compared to the conventional suspensions required many repeated simulations. Thus, simulation time is a critical parameter for the project and the simulations need to give reliable results while having a reasonable run time. For example, the driving distance

clearly affected the response but is only influenced by the characteristics of the road input. Hence, for the same input, the driving distance does not affect a comparison of the dampers. It was chosen to use a simulation time of 20 seconds, which correspond to approximately 390 m of the virtual road. This was thought to be sufficient to capture the characteristics of the different rode types. Regarding the tyre models, the major drawback with the FTire model is the increased simulation time. Even though, it was chosen to use the FTire model in the analysis since it is valid for the high frequencies that affect ride comfort while the PAC2002 model is mainly suitable for low frequency analysis. In conclusion, the parameters defining the comfort analysis are:

Frame Flexible
Sampling frequency 400 Hz
Time 20 s
Velocity 70 km/h
Tyre-model FTire
Solver I3
Computational error $1 \cdot 10^{-3}$

Comfort tests were performed for both virtual roads, representing a well maintained and a badly maintained road. The comfort values are obtained for the filtered accelerations as presented in Section 2.2.2. A low value indicates low accelerations and good ride comfort. The comfort values from the different simulations are used for comparison of the different control systems and the conventional suspensions.

3.3 Handling

The handling features were analysed by performing a single-lane-change. The steering angle was set to 30 degrees and the maneuvers was carried out for different cycle times. The cycle time defines the operation time for the steering wheel input. Two different cycle times were studied; 1 second and 3 seconds and the total run time was 10 seconds to capture some of the oscillations after the lane change was completed. The benchmark test consisted of the features listed in Section 2.3.1, repeated here the for sake of completeness.

- Cab roll angle (Global)
- Cab roll angle (Relative chassis)
- Cab pitch angle
- Lateral acceleration in central of gravity (Cab)
- Lateral acceleration in front axle

The frequencies that affect handling is usually in the range 2-4 Hz and is was therefore chosen to use PAC2002 tyres in the handling study. Apart from the tyre model was the handling analysis carried out using same simulation settings as in the comfort analysis, see below.

Frame Flexible
Sampling frequency 400 Hz
Time 10 s
Cycle time 1 second & 3 seconds
Velocity 70 km/h
Tyre-model FTire
Solver I3
Computational error $1 \cdot 10^{-3}$

3.4 Long dip

The long dip analysis simulates the vehicle when driving through a deep dip in the road and is carried out using the road simulator in Adams/Car. The profile of the virtual road is shown in Figure 3.1. The long dip analysis aims to investigate how well the suspensions perform when there is a sudden obstacle in the road. The input differs significantly from the road vibrations that arise from driving on a flat road. The bump stop and rebound stop are commonly engaged for this type of manoeuvres as a result of large pitch motions of the cab. A good suspension should isolate the cab from vibrations while working to prevent large relative motions between the cab and chassis. Hence, the performance of the suspensions is evaluated based on the contact forces in the bump stop and the rebound stop as well as their displacement.

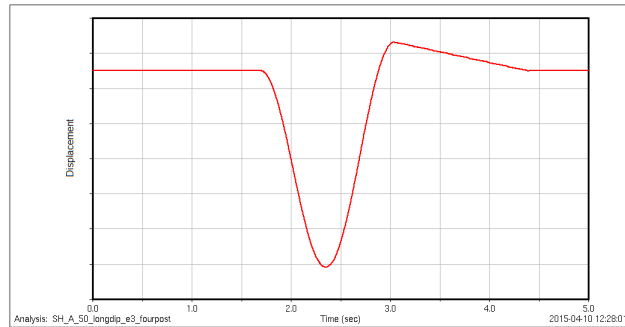


Figure 3.1: *Virtual road profile for a long dip*

The simulations settings are as follows:

Frame Flexible

Sampling frequency 400 Hz

Time 5 s

Velocity 40 km/h

Tyre-model PAC2002

Solver I3

Computational error $1 \cdot 10^{-3}$

4 Controller Design

This chapter provides a presentation on how the different control algorithms were designed and implemented in Adams/Car. Furthermore, different test cases are introduced, which all have a unique set up in terms of control strategy and purpose. The analyses that were performed for each test case are also described.

4.1 Implementation of control system

The control algorithms described in section 2.6 and 2.7 were developed in Matlab/Simulink. The Simulink models were used to generate an External System Library (ESL) file, which is a Adams/Car compliant property file that contains the control algorithm. The ESL-file was then uploaded to a database in Adams. The main advantage with importing control systems in Adams is that simulations are carried out within the Adams environment, i.e. there is no need for co-simulation that invoke other software during simulation, which reduces simulation time.

Some modification of truck assembly was needed in order to successfully implement a control system. The Adams/Mechatronics plug in tool was used to create a subsystem of the controller. The input and output of the control system were defined here. The same signals that donated the input and output signals of the control system were used to define the transducers and actuator signals in the cab subsystem. Accordingly, the input signals to the control system are given by the transducers signals from the cab and the output of the control system acts as actuators signals in the cab subsystem. How the signals are transferred between the subsystems are schematically shown in Figure 4.1. General for all control systems that are studied in this thesis is that the input to the control systems are donated by the upper and lower velocities of the suspensions, i.e. the velocities of the cab and the chassis in each pivot point. The control forces for the front and rear vertical dampers donates the output. Adams/Car measures velocity in millimetre per second (mm/s) and force in Newton (N). It was chosen to use SI units throughout the design of the controller and the control system input, i.e. the velocities, was therefore transformed to meter per second (m/s) in Simulink.

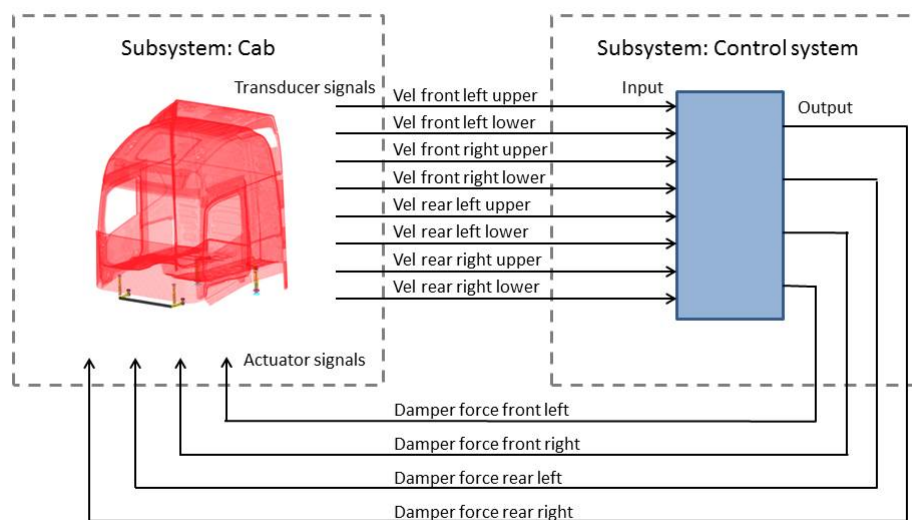


Figure 4.1: Transfer of control signals between the cab subsystems and the control subsystem

The active and semi-active dampers were modelled in Adams/Car by creating a translational force between the upper and lower points of the mounting. The damping forces were controlled by the control system and the assigned control law. When the control system was activate, the passive dampers were deactivated and when the control system was turned off did the original dampers automatically become active.

4.2 No-jerk tuning

The no-jerk algorithm, which is used in semi-active control to create a smooth transition between low state and a high state, is defined by equation 2.80. To increase the performance of the algorithm the parameter v_0 has to be tuned. The performance is evaluated based on how fast the response is and how the applied force complies with the desired force. Additionally, the response needs to be smooth enough to avoid a jerk since a too fast transition induces numerical problems for the solver.

The no-jerk algorithm was evaluated for different v_0 , set to 1 mm/s, 10 mm/s and 100 mm/s. Figure 4.2 shows the response for $v_0 = 1$ mm/s and $v_0 = 100$ mm/s for the time interval 2 – 5 seconds of the badly maintained road, which is representative for the complete simulation. The jerk mitigated forces are presented together with the desired forces to show how the applied force is affected by the no-jerk algorithm and tuning parameter v_0 .

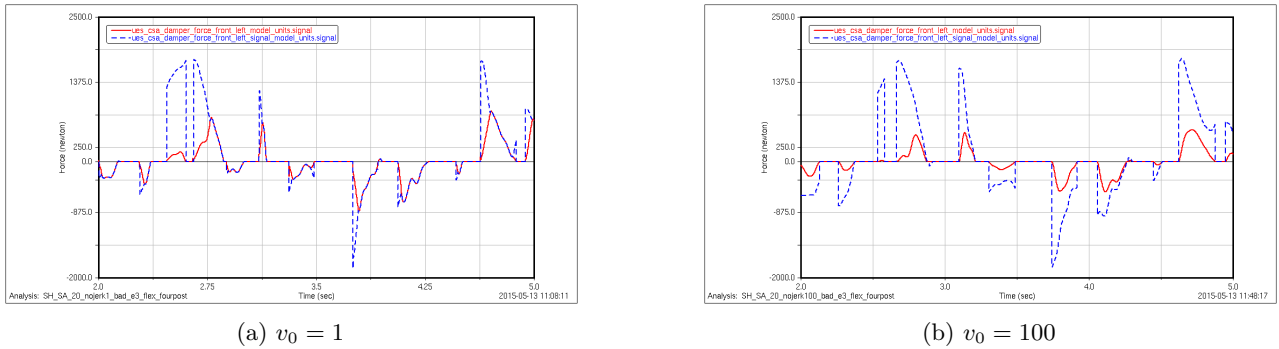


Figure 4.2: Influence of the "No-jerk" algorithm for a) $v_0 = 1$ and b) $v_0 = 100$. The presented control forces correspond to the front left hand side damper and a badly maintained road — — Desired force, — — Applied force

The figures show that the applied force is closer to the desired force for small v_0 , which was expected. What is not seen in the figure is that the solver experienced numerical issues for $v_0 = 1$ mm/s, which is assumed to be an effect of too fast, or jerky, transitions. It was therefore concluded to use $v_0 = 10$ mm/s in all simulations with semi-active control since $v_0 = 10$ mm/s proved to be smooth enough for the solver while still providing a sufficiently fast response. How well the applied force mimic the desired force is affected by the velocity of the cab and the relative velocity over the suspensions. The desired force corresponds to the velocity of the cab and the relative velocity is included in the no-jerk algorithm. A high peak in the desired force is a result of that the cab is moving with high speed. Note that when desired force is nonzero, the velocity of the cab and the relative velocity have the same sign, i.e. moves in the same direction. This is known from the condition corresponding to semi-active control. For the applied force to match the desired force, the relative velocity needs to be sufficiently large to generate the desired damping force.

4.3 Test cases

To be able to organize, plan and perform the simulations in an effective way, a number of test cases were created. Each case has a unique control system and setting and at least one variable damping parameter that controls the damping forces that are applied to the system, e.g. c_{sky} in skyhook control. These damping parameters were varied in order to change the system behaviour and to create different subcases of each test

case. Which coefficients that were studied in each test case are further explained in the following sections. Initially, the variable parameters were changed repeatedly and many shorter simulations were run in both Matlab and Adams/Car and compared to one and other by studying the accelerations and force curves. This was done to estimate the model behaviour and to identify trends and thus, narrow down the range of coefficients for the full-scale study. A limited number of different damping coefficients were then included in the continued analysis.

Six different test cases were designed. Comfort and handling analysis were performed for Case 1-5 and Case 6 comprise an analysis of when the truck model drives through a long dip. The different test cases were studied with the same simulation settings as the benchmark tests, see Section 3, so that all analysis could be compared to the conventional suspension settings.

4.3.1 Case 1 - Active individual skyhook

The active skyhook algorithm was developed according to equation 2.57. In this case, the aim was to suppress the vibration at every suspension point, independently of the movement of the other suspensions and the overall motion of the cab. The control algorithm is straight forward and easy to implement. The Simulink model for one of the suspension points can be seen in Figure 4.3. The complete model is equipped with one controller with the same gain, or coefficient c_{sky} , at each suspension point.

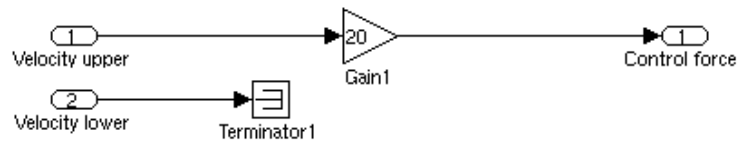


Figure 4.3: Simulink model of the active individual skyhook

The only variable parameter in this case was c_{sky} . Four different comfort analysis was carried out with c_{sky} set to different values according to the subcases in Table 4.1. The handling features were evaluated for subcase 2-4.

| Subcase | c_{sky} [kNs/m] |
|---------|-------------------|
| 1 | 10 |
| 2 | 20 |
| 3 | 50 |
| 4 | 100 |

Table 4.1: Subcases for Case 1 - Active individual skyhook control

4.3.2 Case 2 - Semi-active individual skyhook

The Simulink model for the individual semi-active skyhook control system is seen in Figure 4.4. The control system was, similar to Case 1, designed based on equation 2.75. Semi-active control was obtained according to the condition in equation 2.76, which determines if the system is in high state or low state. The input to the "semi active control" block is the upper velocity, the product of the upper velocity and the relative velocity of the suspension and the ideal damping coefficient c_{sky} . If the product is positive, i.e. when the velocity of the cab and the relative velocity over the suspension have the same sign, the system is in high state. The control force in high state is equal to the upper velocity times the ideal damping coefficient c_{sky} . If the product is negative, the system is in low state and the control force is set to 0. The model also contains a no-jerk module to make the transition between low state and high state continuous. The no-jerk module is described more thoroughly in section 2.8.

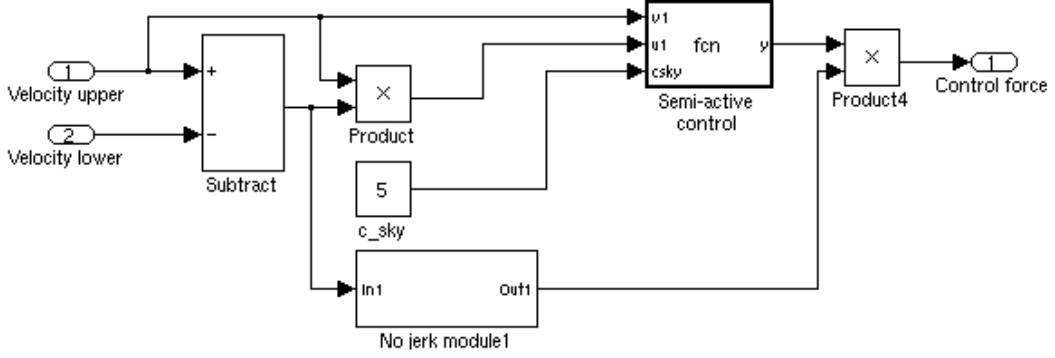


Figure 4.4: Simulink model of the semi-active individual skyhook

It was seen in initial testing that semi-active skyhook performed better for smaller damping coefficients compared to the active control, which is why the coefficients in the test cases differ. The response of the control system for the comfort analysis was studied by varying c_{sky} according to Table 4.2. The handling features were evaluated for subcase 2-4.

| Subcase | c_{sky} [kNs/m] |
|---------|-------------------|
| 1 | 1 |
| 2 | 5 |
| 3 | 10 |
| 4 | 20 |

Table 4.2: Subcases for Case 2 - Semi-active individual skyhook control

4.3.3 Case 3 - Active modal skyhook

Case 3 uses skyhook theory in combination with the modal damping approach to control the motions of the cab. The purpose of this case was mainly to evaluate the influence of c_{roll} and c_{pitch} . c_{heave} was set therefore set to a fixed value while different combinations of roll and pitch coefficients were studied. Three subcases were analysed, see Table 4.3.

| Subcase | c_{heave} [kNs/m] | c_{roll} [kNms/rad] | c_{pitch} [kNms/rad] |
|---------|---------------------|-----------------------|------------------------|
| 1 | 100 | 50 | 50 |
| 2 | 100 | 100 | 50 |
| 3 | 100 | 50 | 100 |

Table 4.3: Subcases for Case 3 - Active modal skyhook

The input to the control system is still, as in individual control, given by the velocities in each suspension point. The modal motions was therefore derived from the suspension velocities, according to 2.37-2.39. This operation is included in the "cog motion calculation". The output from the block is the heave velocity and the roll and pitch angular velocities of the cab. The heave velocity has the unit m/s and the angular velocities are measured in rad/s. The Simulink model can be seen in Figure 4.5. The actual control system is in the "Force distribution" block. The desired forces and torques, acting in the centre of gravity, is determined according to equation 2.59-2.61 and then translated to control forces by solving the system of equations in 2.45.

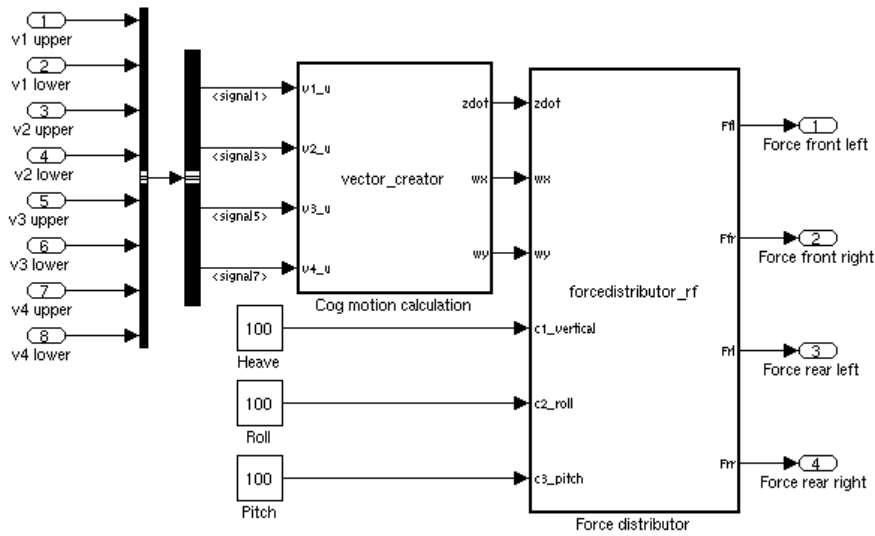


Figure 4.5: Simulink model of the active modal skyhook

4.3.4 Case 4 - Semi-active modal skyhook

Case 4 is designed based on Case 3 but comprises semi-active force control, according to the condition in equation 2.76, as well as the no-jerk algorithm. The Simulink model is shown in Figure 4.6. Just like Case 3, the purpose of this case was to investigate how the roll and pitch coefficients, c_{roll} and c_{pitch} , affects the performance of the control system. The subcases can be seen in Table 4.4.

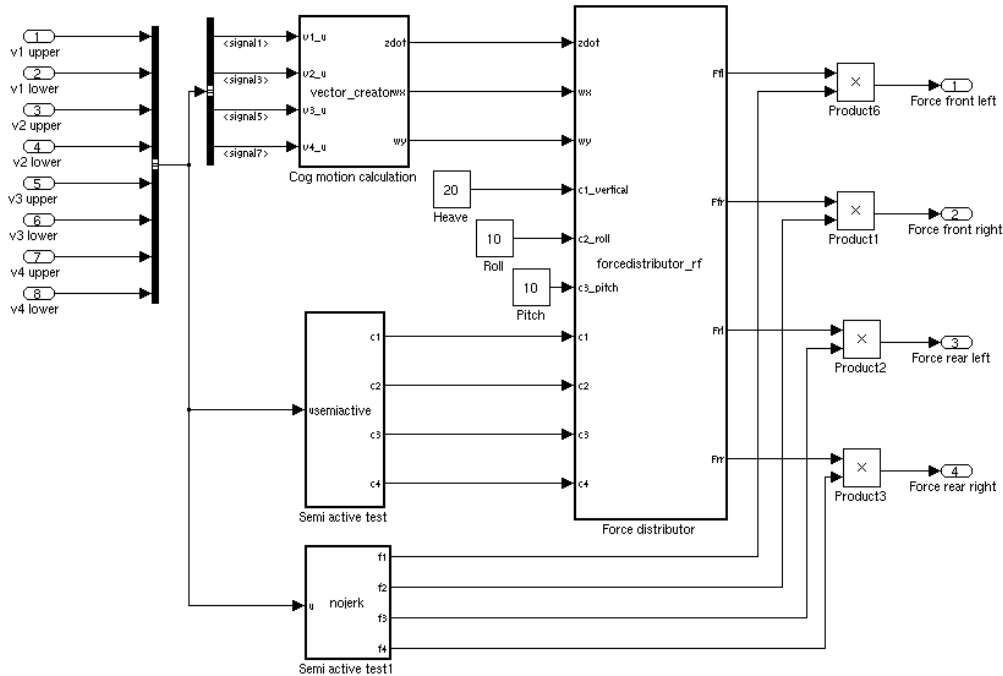


Figure 4.6: Simulink model of the semi-active modal skyhook

| Subcase | c_{heave} [kNs/m] | c_{roll} [kNms/rad] | c_{pitch} [kNms/rad] |
|---------|---------------------|-----------------------|------------------------|
| 1 | 10 | 5 | 5 |
| 2 | 10 | 10 | 5 |
| 3 | 10 | 5 | 10 |

Table 4.4: Subcases for Case 4 - Semi-active modal skyhook

4.3.5 Case 5 - Active LQR

The LQR-control differs from the other control theories but is similar to the modal skyhook control in that sense that the control is based on the modal coordinates. The theory behind LQR control is described in Section 2.6.3 where the state space model of the cab also is presented. To change the behavior of the control system it is possible to vary the weighting matrices \mathbf{Q} and \mathbf{R} . The response of the control system was analysed by setting $\mathbf{R} = \mathbf{R}_0$ and vary the \mathbf{Q} matrix only, to reduce the scope of the study. The elements in \mathbf{R} were kept small to allow large control forces. To investigate the response, simulations were run for three different \mathbf{Q} , which all were based on the matrix \mathbf{Q}_0 . \mathbf{R}_0 and \mathbf{Q}_0 are defined as:

$$\mathbf{R}_0 = \begin{bmatrix} 1 & 0 & 0 & 0 \\ 0 & 1 & 0 & 0 \\ 0 & 0 & 1 & 0 \\ 0 & 0 & 0 & 1 \end{bmatrix} \cdot 10^{-4} \quad (4.1)$$

$$\mathbf{Q}_0 = \begin{bmatrix} 2 & 0 & 0 & 0 & 0 & 0 \\ 0 & 1 & 0 & 0 & 0 & 0 \\ 0 & 0 & 1 & 0 & 0 & 0 \\ 0 & 0 & 0 & 2 & 0 & 0 \\ 0 & 0 & 0 & 0 & 1 & 0 \\ 0 & 0 & 0 & 0 & 0 & 1 \end{bmatrix} \cdot 10^4 \quad (4.2)$$

The LQR control algorithm was initially run for different \mathbf{Q} in a separate Matlab program to solve the Ricatti equation and obtain the gain matrix, \mathbf{G} , by using equations 2.67-2.68. Solving the Ricatti matrix in every time step would be time consuming and thus, this initial analysis saved simulation time once implementing the control in Adams/Car. Since the gain matrix is time independent, this did not affect the outcome. The solution of the Ricatti equation was obtained for the subcases presented in Table 4.5. The gain matrix pertinent to the current subcase and the current state \mathbf{x} was used to determine the optimal control forces in \mathbf{u}_* according to equation 2.66. This operation was implemented in the "lqr active" block in the Simulink model, see Figure 4.7.

| Subcase | \mathbf{Q} | \mathbf{R} |
|---------|------------------|----------------|
| 1 | \mathbf{Q}_0 | \mathbf{R}_0 |
| 2 | $10\mathbf{Q}_0$ | \mathbf{R}_0 |
| 3 | $20\mathbf{Q}_0$ | \mathbf{R}_0 |

Table 4.5: Subcases for active LQR

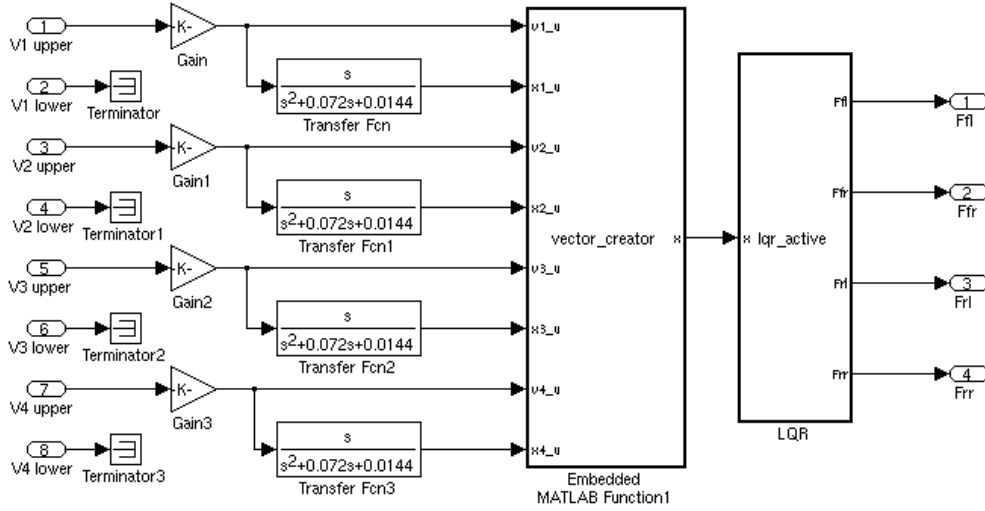


Figure 4.7: Simulink model of the LQR control

The same template for the control system was used as for in the other cases, i.e. had the same input and output signals. The positions of the upper suspensions points were obtained through integration of the velocities. The integration was performed with a pseudo integrator on the form

$$I = \frac{s}{s^2 + 2\zeta\omega s + \omega^2} \quad (4.3)$$

where $\omega = 0.1 \text{ Hz} = 0.12 \text{ rad/s}$ and $\zeta = 0.3$. These parameter values were selected to achieve a good behaviour in the range of interest [7]. The filter function is a combination of high pass filter and an integrator, see Figure 4.8. Furthermore, advantages with using the integrated velocities to obtain the positions is that the static displacement is removed and also that the same control template could be utilized.

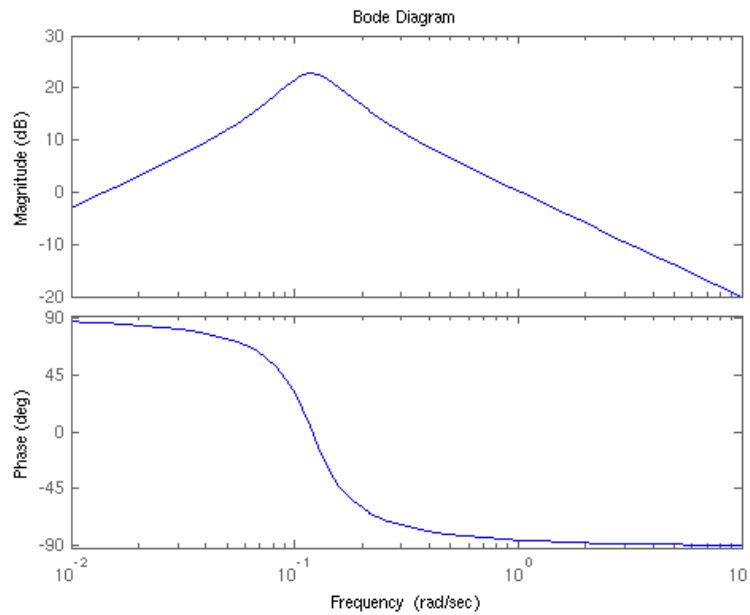


Figure 4.8: Pseudo integrator - Filter function and phase

4.3.6 Case 6 - Long dip

The long dip simulation was performed for the individual active and semi-active skyhook controllers, for two subcases each. The chosen subcases correspond to damping coefficients that showed good performances in the comfort analysis. This type of road profile commonly induces large pitch motions of the cab, which creates large displacements of the cab relative to the chassis. This in turn engages the bump and rebound stop if the relative motion is too large. It is therefore interesting to study the displacement and contact forces in the bump and rebound stops to evaluate the performance of the cab suspensions. The subcases used in the long dip analysis are seen in Table 4.6.

| Control system | Subcase | c_{sky} |
|---------------------|---------|-----------|
| Active skyhook | 1 | 20 |
| | 2 | 50 |
| Semi-active skyhook | 3 | 5 |
| | 4 | 10 |

Table 4.6: Subcases for Case 6

5 Results

In this chapter are the results from the different test cases and simulations that was described in section 4.3 presented and evaluated.

5.1 Case 1 - Active individual skyhook

Case 1 is represented by active individual skyhook control. Here are the results from the analysis presented and evaluated.

5.1.1 Comfort

The focus of the comfort analysis was to investigate how the vibrations in cab are influenced by varying damping coefficients, c_{sky} , with the objective to improve the ride comfort. Good comfort is characterised by a low comfort value and the performance of the control system is therefore evaluated based on how much the comfort value can be reduced through the use of the control system. How the implementation of the different subcases with active individual skyhook control affects the comfort value compared to the benchmark tests is shown in Table 5.1. The table includes the results from the comfort analysis of a badly maintained and a less maintained road, i.e. high and low road vibrations respectively.

| Control system | Subcase | c_{sky} [kNs/m] | Comfort value, change [%] | |
|---------------------------------|---------|----------------------|---------------------------|------|
| | | | Badly | Less |
| Active skyhook, ind. control | 1 | 10 | -22 | -32 |
| | 2 | 20 | -27 | -32 |
| | 3 | 50 | -27 | -32 |
| | 4 | 100 | -23 | -29 |

Table 5.1: Change of the comfort values compared to the benchmark tests for active individual skyhook control with different ideal damping coefficients c_{sky} . The results correspond to analysis with a badly maintained road and a less maintained road.

It is seen that the active individual skyhook control significantly improves the performance in terms of comfort. It is not possible to determine an optimal damping coefficient from this range of values and road data only but it is possible to identify trends in the system behaviour. The largest improvement is obtained from simulations with a less maintained road that corresponds to low road vibrations. The best results correspond to a reduction of the comfort value with 32 %, which is obtained for several of the subcases. In simulations with high road vibrations, i.e. a badly maintained road, the best result shows an improvement of 27 %, which is obtained for both $c_{sky} = 20$ kNs/m and $c_{sky} = 50$ kNs/m. The comfort value increases if looking in intervals below 20 kNs/m and over 50 kNs/m.

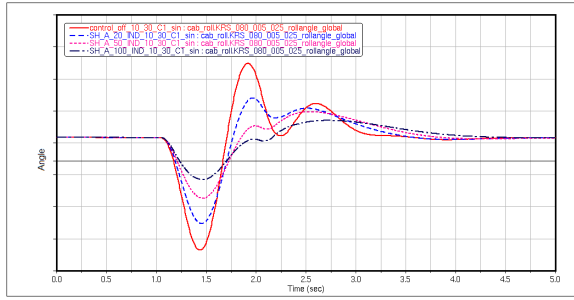
The larger the damping coefficient is, the larger are the forces that are induced in the system. The maximum force measured in any of the actuators during the analysis is shown in Table 5.2. The maximum force an active damper can provide is obviously restricted by the properties of the actuator and the power supply. The larger the desired forces are, the more powerful and thus, more power consuming and expensive system is required. With the objective to minimize the energy consumption and to achieve good performance for both low and high vibration input, the results points to that c_{sky} at least should be between 10 – 20 kNs/m.

| Control system | Subcase | c_{sky} [kNs/m] | Max. damping force [kN] | |
|---------------------------------|---------|----------------------|-------------------------|------|
| | | | Badly | Less |
| Active skyhook, ind. control | 1 | 10 | 2.3 | 0.49 |
| | 2 | 20 | 2.9 | 0.70 |
| | 3 | 50 | 3.9 | 1.0 |
| | 4 | 100 | 4.8 | 1.2 |

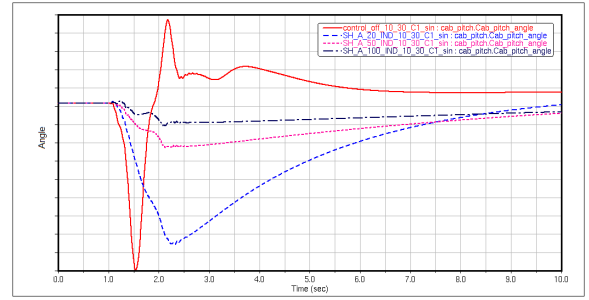
Table 5.2: Maximum damping force, using active individual skyhook control with different ideal damping coefficients c_{sky}

5.1.2 Handling

Figure 5.1 and Figure 5.2 shows the global cab roll angle and the cab pitch angle from the handling analysis. The figures includes the benchmark test and the test case using $c_{sky} = 20, 50$ and 100 kNs/m. The figures show that the roll angle decreases but the time delay between the steering angle and the roll response grows as c_{sky} increases. This becomes more evident for longer cycles, see Figure 5.2a. This delay can make it harder for the driver to interpret the behaviour of the truck. The phenomenon is explained by increased damping in the system. For large c_{sky} it is seen that the system even becomes over damped. Increased damping results in an overall slower system as the active damper is working to minimize the motion of the cab. The figures also show that the pitch motion also decrease with the active control system and increasing c_{sky} due to increased damping forces.



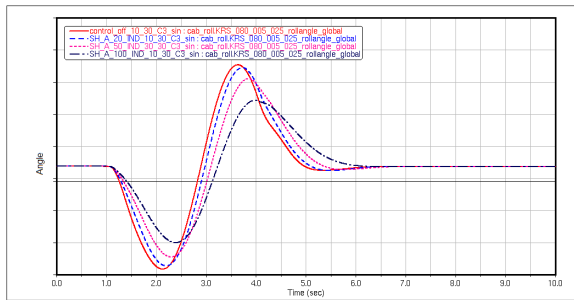
(a) Cab roll angle, global



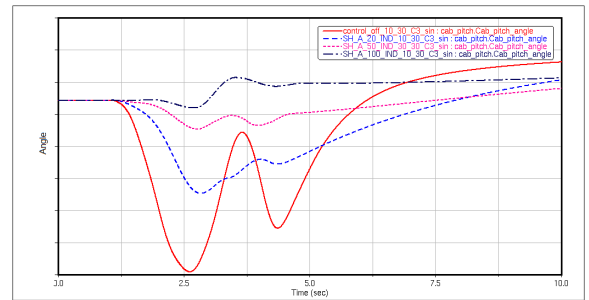
(b) Cab pitch angle

Figure 5.1: a) Global cab roll angle and b) cab pitch angle for the benchmark test and individual active skyhook control with different ideal damping coefficients c_{sky} , for 1 second long cycle.

— Benchmark, — $c_{sky} = 20$ kNs/m, ··· $c_{sky} = 50$ kNs/m, -·- $c_{sky} = 100$ kNs/m



(a) Cab roll angle, global



(b) Cab pitch angle

Figure 5.2: a) Global cab roll angle and b) cab pitch angle for the benchmark test and individual active skyhook control with different ideal damping coefficients c_{sky} , for 3 seconds long cycle.

— Benchmark, — $c_{sky} = 20$ kNs/m, ··· $c_{sky} = 50$ kNs/m, -·- $c_{sky} = 100$ kNs/m

As established, the global roll angle decrease for increasing c_{sky} . However, stabilizing the cab through active skyhook control involves large forces that act between the cab and the chassis. This results in that the chassis experience large excitation forces that result in increased motions, which in turn leads to that the relative roll angle of the cab grows with increasing c_{sky} . Figure 5.3 shows the cab roll angle relative to the chassis for the longer of the two cycles, for which the described behaviour is more evident.

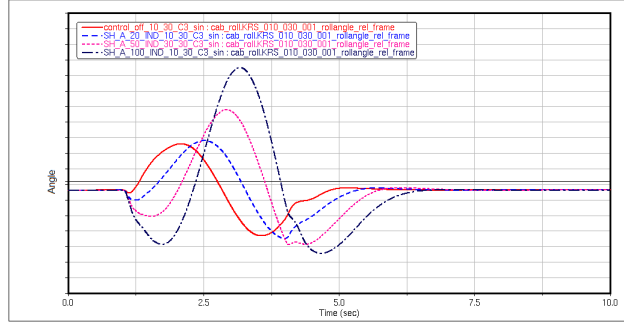
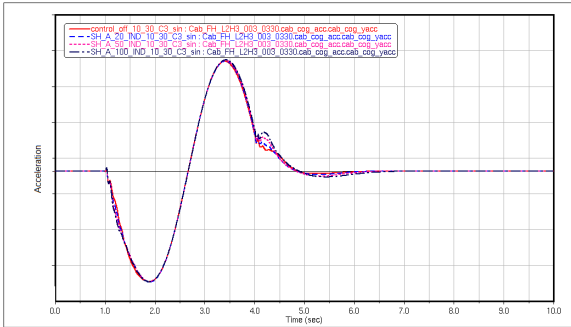
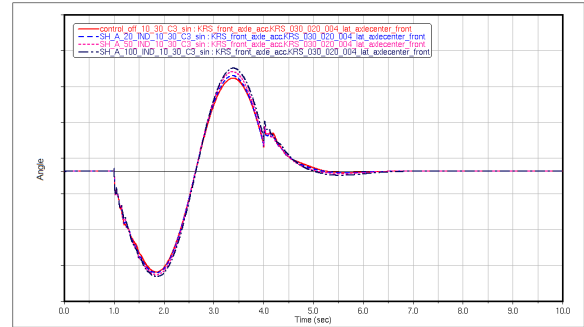


Figure 5.3: Cab roll angle relative chassis for the benchmark test and active skyhook control with different ideal damping coefficients c_{sky} , for 3 seconds long cycle. — Benchmark, - - $c_{sky} = 20$ kNs/m, ···· $c_{sky} = 50$ kNs/m, - · - $c_{sky} = 100$ kNs/m

The lateral accelerations in the centre of gravity and in the front axle are also studied and the response is presented for the 3 seconds long cycle in Figure 5.4. There is a small increase of the lateral acceleration in the front axle for increasing c_{sky} but the behaviour is overall virtually unaffected by the integration of the active control system.



(a) Center of gravity of the cab



(b) Front axle

Figure 5.4: Lateral accelerations in a) the center of gravity and b) the front axle for the benchmark test and individual active skyhook control with different ideal damping coefficients c_{sky} , for 3 seconds long cycle. — Benchmark, - - $c_{sky} = 20$ kNs/m, ···· $c_{sky} = 50$ kNs/m, - · - $c_{sky} = 100$ kNs/m

5.2 Case 2 - Semi-active individual skyhook

Case 2 is represented by semi-active individual skyhook control. Here are the results from the analysis presented and evaluated.

5.2.1 Comfort

The results from the comfort analysis with a badly maintained and a less maintained road are shown in Table 5.3. The analysis with low road vibrations shows a clear improvement of the comfort value. The results for a badly maintained road also points to improved comfort but not in the same order. Compare the reduction of the comfort value of 10 % for high vibration input and 21 % for low road vibrations. The characteristics of the response are similar in terms of where the optimal value is found. The best result is obtained for $c_{sky} = 5$ kNs/m for both road qualities. This indicates that there is, at least, a local optimum for c_{sky} that generates to the best performance independent of road severity. However, this is not feasible to conclude from simulations with only two different kinds of road qualities.

| Control system | Subcase | c_{sky} [kNs/m] | Comfort value, change [%] | |
|-----------------------------------|---------|----------------------|---------------------------|------|
| | | | Badly | Less |
| Semi-active skyhook, ind. control | 1 | 1 | +0 | -14 |
| | 2 | 5 | -10 | -21 |
| | 3 | 10 | -5.0 | -18 |
| | 4 | 20 | +5.0 | -11 |

Table 5.3: Change of the comfort values compared to the benchmark tests for active individual skyhook control with different ideal damping coefficients c_{sky} .

The maximum damping force for the different subcases is seen in Table 5.4. The forces supplied by the semi-active control system are generally lower compared to active control forces for the same damping coefficient. Semi-active control can be achieved with minimal energy consumption but is less powerful than an active system since the damping force is more restricted. Moreover, the no-jerk algorithm, which creates a continuous transition from low state to high state further decreases the applied force compared to the desired force, see Figure 4.2. An example of the characteristics of the applied force for active and semi-active dampers is seen in Figure 5.5. As no large-scale external energy source is needed for semi-active control systems, the maximum damping force should be viewed more as a dimensioning parameter for the system than an indicator of the power consumption.

| Control system | Subcase | c_{sky} [kNs/m] | Max. damping force [kN] | |
|------------------------------|---------|----------------------|-------------------------|------|
| | | | Badly | Less |
| Active skyhook, ind. control | 1 | 1 | 0.4 | 0.16 |
| | 2 | 5 | 1.5 | 0.36 |
| | 3 | 10 | 1.6 | 0.50 |
| | 4 | 20 | 2.2 | 0.63 |

Table 5.4: Maximum damping force, using semi-active individual skyhook control with different ideal damping coefficients c_{sky}

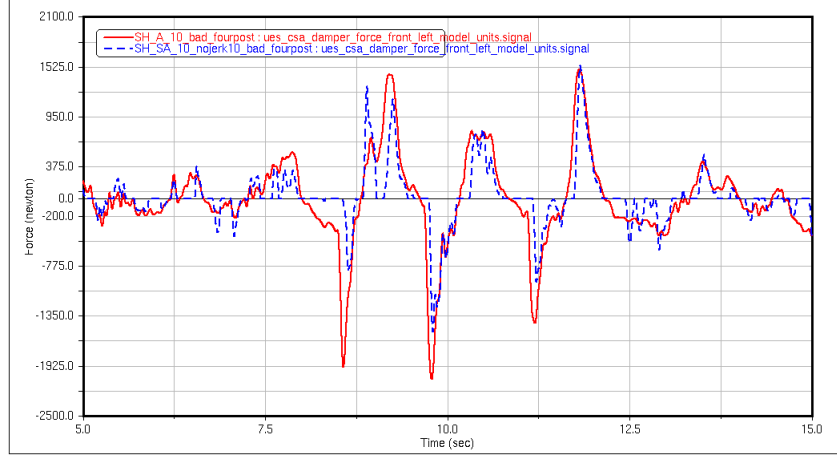
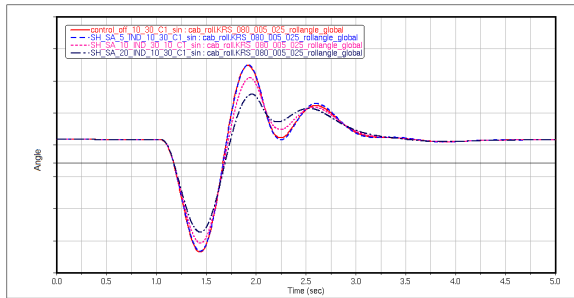


Figure 5.5: Applied force by the front left damper by the active and semi-active skyhook control systems for $c_{sky} = 10 \text{ kNs/m}$ and badly maintained road input. — Active skyhook, - - Semi-active skyhook

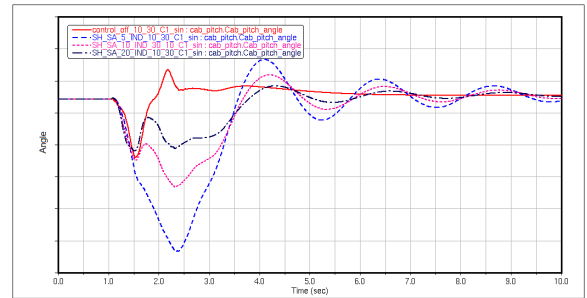
5.2.2 Handling

The results from the handling analysis in terms of the the global roll angle and pitch angle are shown in Figure 5.6 and Figure 5.7. The handling analysis for the 1 second cycle shows that it's possible decrease the roll angle and the pitch angle by increasing c_{sky} . The improvement is smaller compared to the active case, which is due to the fact that semi-active controllers are less powerful. Figure 5.7a presents the roll angle for the 3 second cycle and it is seen that the roll angle barely changes as c_{sky} increases. This can be explained by that neither c_{sky} or the roll velocity are sufficiently large for the induced forces to have an impact. For a quicker manoeuvre, it is seen that the roll velocity becomes large enough to trigger the anti-roll torque, see Figure 5.6a.

Both Figure 5.6b and Figure 5.7b, which display the pitch angle for the handling analysis, shows that the system becomes under damped for all values of c_{sky} . This results in undesired oscillations of the cab that continues after the manoeuvre is finished. This is also an effect of lacking damping forces due to the combination of small damping coefficients and small suspension velocities.



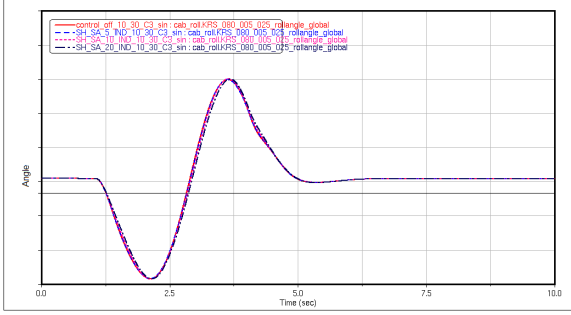
(a) Cab roll angle, global



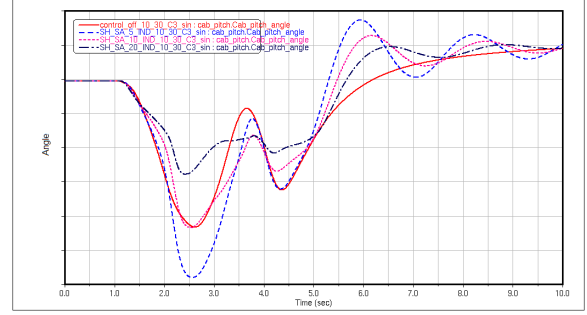
(b) Cab pitch angle

Figure 5.6: a) Global cab roll angle and b) cab pitch angle for the benchmark test and individual semi-active skyhook control with different ideal damping coefficients c_{sky} , for 1 second long cycle.

— Benchmark kNs/m , - - $c_{sky} = 5 \text{ kNs/m}$, - - - $c_{sky} = 10 \text{ kNs/m}$, - - - - $c_{sky} = 20 \text{ kNs/m}$



(a) Cab roll angle, global



(b) Cab pitch angle

Figure 5.7: a) Global cab roll angle and b) cab pitch angle for the benchmark test and individual semi-active skyhook control with different ideal damping coefficients c_{sky} , for 3 seconds long cycle.

— Benchmark, - - $c_{sky} = 5 \text{ kNs/m}$, - - - $c_{sky} = 10 \text{ kNs/m}$, - - - $c_{sky} = 20 \text{ kNs/m}$

Figure 5.8 shows the relative roll angle for the longer of the two maneuvers, i.e. for the 3 seconds cycle. Different from the active case, its not significantly affected by the implementation of the semi-active control systems. The lateral acceleration in the center of gravity and front axle is similar to Case 1 unaffected by the implementation of control system and therefore not presented.

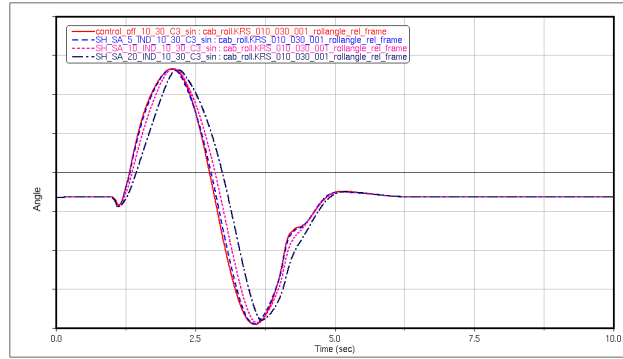


Figure 5.8: Cab roll angle relative chassis for the benchmark test and semi-active skyhook control with different ideal damping coefficients c_{sky} , for 3 seconds long cycle. — Benchmark, - - $c_{sky} = 5 \text{ kNs/m}$, - - - $c_{sky} = 10 \text{ kNs/m}$, - - - $c_{sky} = 20 \text{ kNs/m}$

5.3 Case 3 - Active modal skyhook

Case 3 is represented by active modal skyhook control. Here are the results from the analysis presented and evaluated.

5.3.1 Comfort

The result from the comfort analysis and the different subcases is seen in Table 5.5 and the corresponding maximum damping forces, applied by any of the actuators, is seen in Table 5.8. The output shows that the active modal skyhook control performs well for both road qualities. By comparing the reduction of the comfort values in relation to the maximum damping forces, it is found that the system behaviour of the individual and modal control strategies is similar but that there is a small difference in the results. All subcases with modal control show at least equivalent or improved comfort compared to the case with individual active skyhook, which indicates that it is possible to achieve better performance with the modal control strategy.

The influence of the damping parameters is small, in particular in simulations with a less maintained road for which the comfort value is unaffected by the variation of roll and pitch coefficients. In simulations with a badly maintained road, the best result corresponds to subcase 3 for which the pitch coefficient is increased. The improvement is a result of reduced longitudinal accelerations compared to subcase 1. Notice that the maximum damping force is not significantly affected by the increased pitch coefficient while increasing the roll parameter leads to increasing damping forces.

| Control system | Subcase | c_{sky} [kNs/m] | c_{roll} [kNms/rad] | c_{pitch} [kNms/rad] | Comfort value, change [%] | |
|-------------------------------|---------|----------------------|--------------------------|---------------------------|---------------------------|------|
| | | | | | Badly | Less |
| Active skyhook, modal control | 1 | 100 | 50 | 50 | -27 | -36 |
| | 2 | 100 | 100 | 50 | -25 | -36 |
| | 3 | 100 | 50 | 100 | -28 | -36 |

Table 5.5: Comfort values for active modal skyhook control with different coefficients c_{sky} , c_{roll} and c_{pitch} , compared to the benchmark tests.

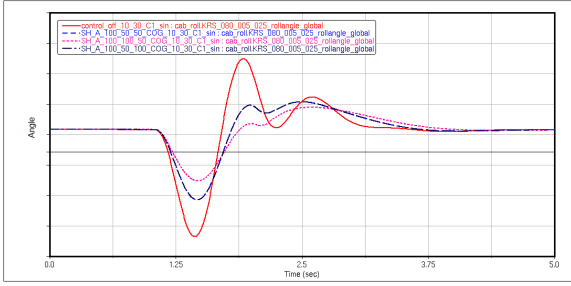
| Control system | Subcase | c_{sky} [kNs/m] | c_{roll} [kNms/rad] | c_{pitch} [kNms/rad] | Max. damping force [kN] | |
|-------------------------------|---------|----------------------|--------------------------|---------------------------|-------------------------|------|
| | | | | | Badly | Less |
| Active skyhook, modal control | 1 | 100 | 50 | 50 | 3.2 | 0.81 |
| | 2 | 100 | 100 | 50 | 3.6 | 0.99 |
| | 3 | 100 | 50 | 100 | 3.3 | 0.83 |

Table 5.6: Maximum damping force, using active modal skyhook control with different coefficients c_{sky} , c_{roll} and c_{pitch}

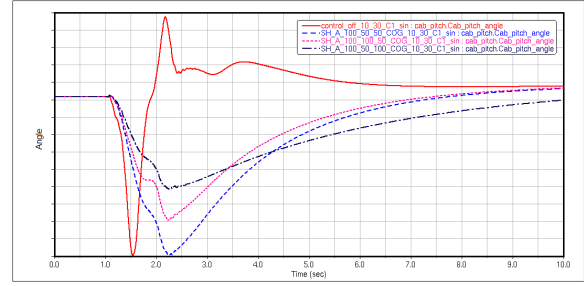
5.3.2 Handling

The results from the handling analysis, 1 second and 3 seconds cycles, is seen in Figure 5.9 and Figure 5.10 respectively. In Figure 5.9a it is seen that only increasing c_{roll} by a factor two results in a smaller roll angle and that a doubling of c_{pitch} does not visibly affect the response. If looking at the pitch angle in Figure 5.9b, it is seen that both subcases where the roll and pitch coefficient are increased by a factor of two, one at the time, results in decreased pitch motions compared to subcase 1.

The response for both the faster and slower manoeuvre indicates that, even though the roll angle decreases, the time delay grows as the damping in the system increases. The system behaviour shows major similarities with the response from the case with individual active skyhook control. The relative roll angle and the lateral accelerations in the cab and in the front axle are not presented here, but it holds that the relative roll angle increases with increased damping and that the lateral accelerations are visually unaffected by the substitution of the conventional dampers.

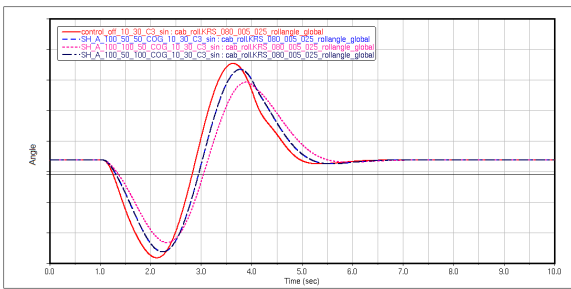


(a) Cab roll angle, global

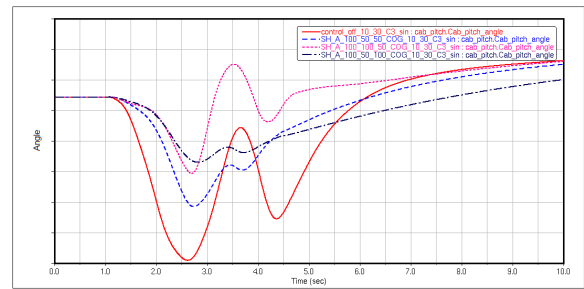


(b) Cab pitch angle

Figure 5.9: a) Global cab roll angle and b) cab pitch angle for the benchmark test and active modal skyhook with different coefficients c_{sky} , c_{roll} and c_{pitch} , for 1 second long cycle. — Benchmark, - - subcase 1, ···· subcase 2, - · - subcase 3



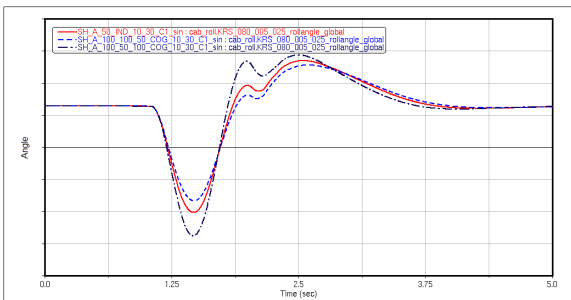
(a) Cab roll angle, global



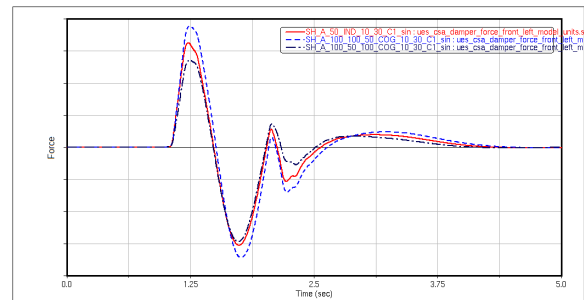
(b) Cab pitch angle

Figure 5.10: a) Global cab roll angle and b) cab pitch angle for the benchmark test and active modal skyhook with different coefficients c_{sky} , c_{roll} and c_{pitch} , for 3 seconds long cycle. — Benchmark, - - subcase 1, ···· subcase 2, - · - subcase 3

The global roll angle for case 1 and case 3 is compared in Figure 5.11a and Figure 5.11b shows the pertinent control forces on the front left hand side of the cab. The behaviour of the different control strategies is very similar. Furthermore, it is seen that the roll angle have a strong correlation to the applied damping force. The curves indicate that the control strategies are likely to give close to equivalent results if the damping parameters were tuned to supply equally large forces.



(a) Cab roll angle, global



(b) Control force, front left hand side

Figure 5.11: a) Global cab roll angle and b) control force for individual control and modal control, for 1 second long cycle. — Active individual skyhook $c_{sky} = 50$ kNs/m, - - subcase 2, - · - subcase 3

5.4 Case 4 - Semi-active modal skyhook

Case 4 is represented by semi-active modal skyhook control. Here are the results from the analysis presented and evaluated.

5.4.1 Comfort

The result from the comfort analysis is presented in Table 5.7. The output is similar to the results that were obtained in Case 2 if comparing the comfort in relation to approximate the same maximum damping forces, see Table 5.8. As in the case with modal active control, the effect of varying the damping parameters is small, especially in simulations with low road vibrations. Here, the best result from the analysis with high road vibrations is obtained for subcase 2, for which the roll coefficient is increased. The control algorithm for this case generated a jerky response, resulting from that the system frequently switched back and forth between low state and high state. This increased the simulation time with a factor of 2-3 compared to individual control. Obviously this is a great flaw with the control, even though the comfort is improved.

| Control system | Subcase | c_{sky} [kNs/m] | c_{roll} [kNms/rad] | c_{pitch} [kNms/rad] | Comfort value, change [%] | |
|------------------------------------|---------|----------------------|--------------------------|---------------------------|---------------------------|------|
| | | | | | Badly | Less |
| Semi-active skyhook, modal control | 1 | 10 | 5 | 5 | -5.0 | -18 |
| | 2 | 10 | 10 | 5 | -10 | -18 |
| | 3 | 10 | 5 | 10 | -8.3 | -18 |

Table 5.7: Comfort values for semi-active modal skyhook control with different coefficients c_{sky} , c_{roll} and c_{pitch} , compared to the benchmark test.

| Control system | Subcase | c_{sky} [kNs/m] | c_{roll} [kNms/rad] | c_{pitch} [kNms/rad] | Max. damping force [kN] | |
|------------------------------------|---------|----------------------|--------------------------|---------------------------|-------------------------|------|
| | | | | | Badly | Less |
| Active semi-skyhook, modal control | 1 | 10 | 5 | 5 | 0.82 | 0.23 |
| | 2 | 10 | 10 | 5 | 0.88 | 0.27 |
| | 3 | 10 | 5 | 10 | 0.83 | 0.26 |

Table 5.8: Maximum damping force, using semi-active modal skyhook control with different coefficients c_{sky} , c_{roll} and c_{pitch}

5.4.2 Handling

The handling features that are affected by the implementation of the modal semi-active control system are the cab roll and pitch motions, which are shown in Figure 5.12 and Figure 5.12.

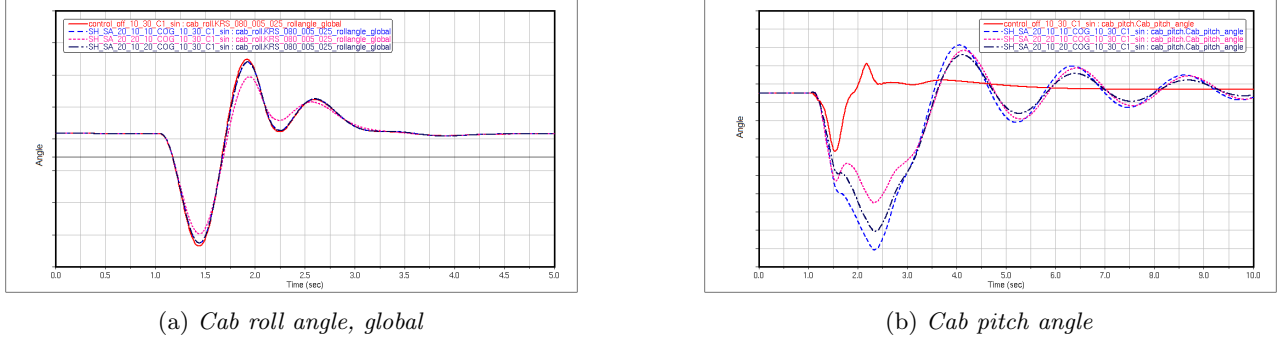


Figure 5.12: a) Global cab roll angle and b) cab pitch angle for the benchmark test and semi-active modal skyhook with different coefficients c_{sky} , c_{roll} and c_{pitch} , for 1 second long cycle. — Benchmark, - - subcase 1, - - - subcase 2, - - - subcase 3

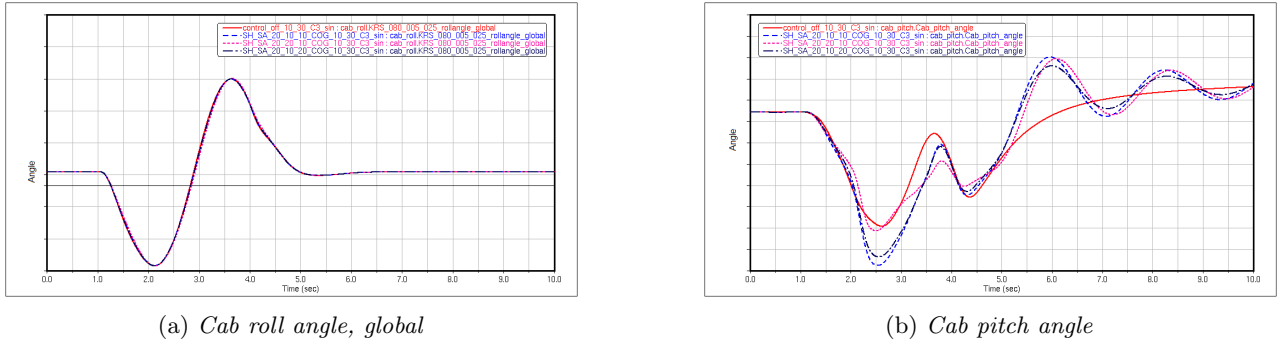
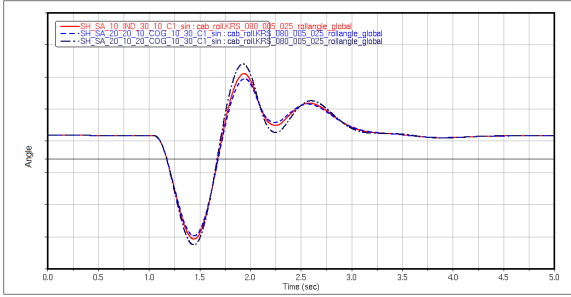


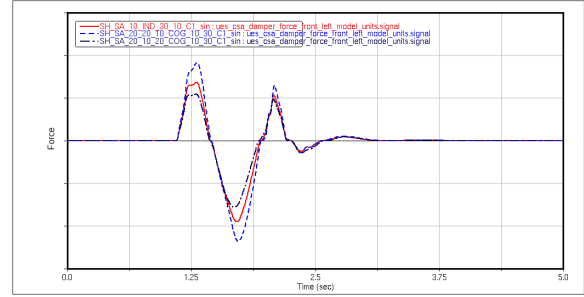
Figure 5.13: a) Global cab roll angle and b) cab pitch angle for the benchmark test and semi-active modal skyhook with different coefficients c_{sky} , c_{roll} and c_{pitch} , for 3 seconds long cycle. — Benchmark, - - subcase 1, - - - subcase 2, - - - subcase 3

The global roll angle and pitch angle for the faster manoeuvre are shown in Figure 5.12. Likewise the active modal control, it is seen that only increasing c_{roll} by a factor two results in a smaller roll angle and that doubling c_{pitch} does not visibly affect the response. Regarding the pitch motions, oscillations of the cab are induced that continue after the manoeuvre is completed. This type of characteristic response was also seen for individual semi-active control and indicates that the system is under damped. Aside from the oscillations, subcase 2, for which the roll coefficient is doubled, shows better results compared to subcase 3 where the pitch coefficient is increased. This is explained by that this kind of manoeuvre generates larger roll motions compared to pitch motions. Thus, increasing the roll coefficient c_{roll} results in overall larger actuator forces, which suppresses all motions of the cab. For a slower manoeuvre, it is seen that the different control systems have small influence on the roll angle, see Figure 5.13a. Regarding the pitch angle, which are shown in Figure 5.13b, the same type of response is obtained as for the faster cycle.

A comparison of the different control strategies, concerning the roll angle and the control forces, is shown in figure 5.15. The comparison includes semi-active individual control with $c_{sky} = 10$ kNs/m and semi-active modal skyhook for subcase 2-3. Subcase 2 shows better performance compared to the individual control. However, this subcase also generates larger damping forces compared to the individual skyhook. It is seen once more that there is a strong correlation between the roll angle and the control forces.



(a) Cab roll angle, global



(b) Control force, front left hand side

Figure 5.14: a) Global cab roll angle and b) control force for individual control och modal control, for 1 second long cycle. — Semi-active individual skyhook $c_{sky} = 10$ kNs/m, - - subcase 2, - · - subcase 3

5.5 Case 5 - Active LQR

Case 5 is represented by LQR. Here are the results from the analysis presented and evaluated.

5.5.1 Comfort

The result shows a significant improvement of the comfort value for the LQR method, see Table 5.9. This indicates that the state space model, upon which the control algorithm is based, as well as the penalty matrices \mathbf{Q} and \mathbf{R} are designed in a good way. The different subcases shows equivalent results in terms of reduction of the comfort value in analysis with a less maintained road. For simulations with a badly maintained road, there is a change between subcase 1 and subcase 2, showing improved comfort for increased damping forces. The maximum damping force applied by any of the actuators is shown in Table 5.10. The relation between comfort and the magnitude of the maximum damping force is consistent to what is seen in the studies of the other active control systems.

| Control system | Subcase | \mathbf{Q} | \mathbf{R} | Comfort value, change [%] | |
|----------------|---------|------------------|----------------|---------------------------|------|
| | | | | Badly | Less |
| Active LQR | 1 | \mathbf{Q}_0 | \mathbf{R}_0 | -18 | -32 |
| | 2 | $10\mathbf{Q}_0$ | \mathbf{R}_0 | -27 | -32 |
| | 3 | $20\mathbf{Q}_0$ | \mathbf{R}_0 | -27 | -32 |

Table 5.9: Comfort values for LQR with different weight matrices \mathbf{Q} , compared to the benchmark tests

| Control system | Subcase | \mathbf{Q} | \mathbf{R} | Max. damping force [kN] | |
|----------------|---------|------------------|----------------|-------------------------|------|
| | | | | Badly | Less |
| Active LQR | 1 | \mathbf{Q}_0 | \mathbf{R}_0 | 1.8 | 0.40 |
| | 2 | $10\mathbf{Q}_0$ | \mathbf{R}_0 | 2.9 | 0.82 |
| | 3 | $20\mathbf{Q}_0$ | \mathbf{R}_0 | 3.2 | 0.97 |

Table 5.10: Maximum damping force, using LQR with different weight matrices \mathbf{Q}

5.5.2 Handling

The response from the handling analysis is very similar to the response obtained for the active skyhook strategies. The result is therefore only presented as a comparison between the LQR method and active individual skyhook control for the 1 second cycle, see Figure 5.15. The handling analysis shows that the roll angle decreases with increasing \mathbf{Q} , i.e. increasing control forces. Smaller roll angles would likely be obtained with the LQR if the generated damping forces were increased further. Overall, the results show that the different control algorithms behave similarly when performing a single lane change.

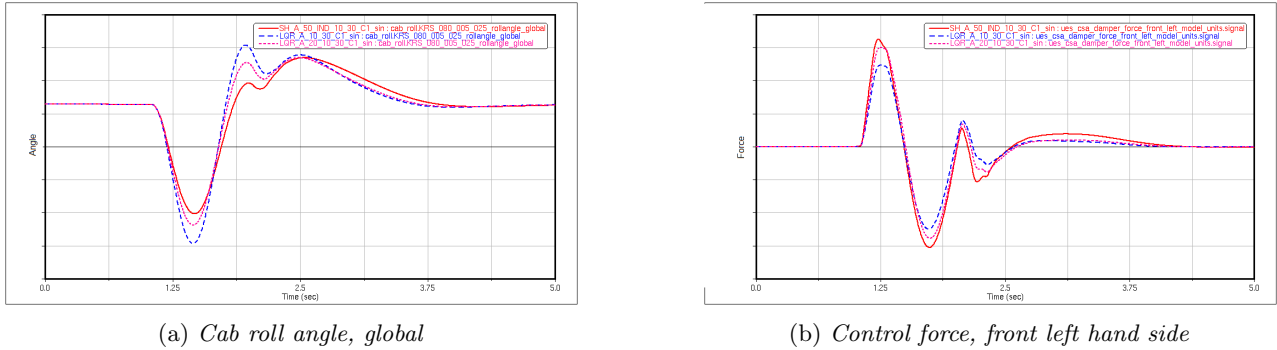


Figure 5.15: a) Global cab roll angle and b) control force for individual active skyhook control och active LQR control, for 1 second long cycle. — Active individual skyhook $c_{sky} = 50$ kNs/m, - - LQR $10\mathbf{Q}_0$, ··· LQR $20\mathbf{Q}_0$

5.6 Case 6 - Long dip

The long dip was analyzed using both active and semi-active individual skyhook control, two subcases for each controller. The chosen subcases show good performances in the comfort analysis. The results from the long dip simulations are presented below.

5.6.1 Active individual skyhook

The long dip analysis are for the active individual skyhook control performed with c_{sky} set to 20 kNs/m and 50 kNs/m. The results from the test case and the benchmark test are presented for the suspension on the rear left hand side and include the displacement of the bump and rebound stop as well as the resultant contact forces, see Figure 5.16 and Figure 5.17. The active system results in larger displacements and forces compared to the conventional system and the larger the ideal damping coefficient c_{sky} , the larger is the displacement of the bump and rebound stop. These problems occur as the control system wants to keep the cab in its original horizontal plane. For example, when the cab travels downhill in the long dip, the control system wants to keep the cab in its initial state by applying a positive damping force vertical direction, in the opposite direction of the motion of the cab. Consequently, the cab is forced upwards and the chassis is forced downwards. Thus, the relative distance between the cab and the chassis increases and eventually, the rebound stop engage. The control system continues to try and push the cab upwards while the rebound stop tries to force it downwards by applying a force in the opposite direction of the damping force. This gives large internal forces acting in the opposite direction, which clearly is not a desirable system response.

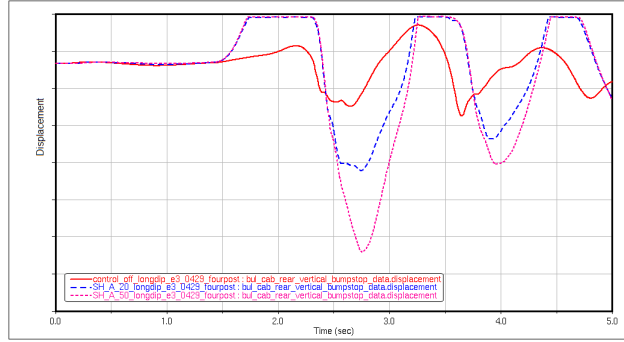
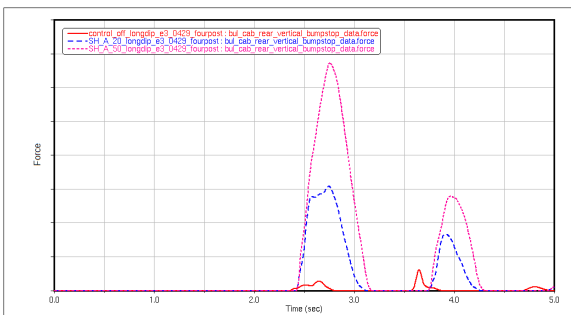
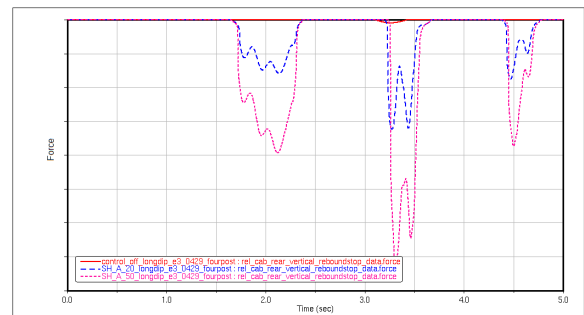


Figure 5.16: Displacements of the bump stop and rebound stop for the benchmark test and for active skyhook control. — Benchmark kNs/m , - - $c_{sky} = 20$ kNs/m , ··· $c_{sky} = 50$ kNs/m



(a) Bump stop forces, rear left hand side



(b) Rebound stop forces, rear left hand side

Figure 5.17: Forces in the a) bump stop and b) rebound stop for the benchmark test and for active skyhook control. — Benchmark kNs/m , - - $c_{sky} = 20$ kNs/m , ··· $c_{sky} = 50$ kNs/m

5.6.2 Semi-active individual skyhook

The result from the long dip analysis using individual semi-active control is displayed for the suspension on the rear left hand side. The displacement of the bump stops and rebound stops as well as the resulting forces are shown in Figure 5.18 and Figure 5.19 respectively. They include the benchmark test and semi-active skyhook control with $c_{sky} = 5$ kNs/m and $c_{sky} = 10$ kNs/m . The same type of behaviour is seen as in the subcases with active control. The response is improved slightly but this is just due to a less powerful system and lower internal forces.

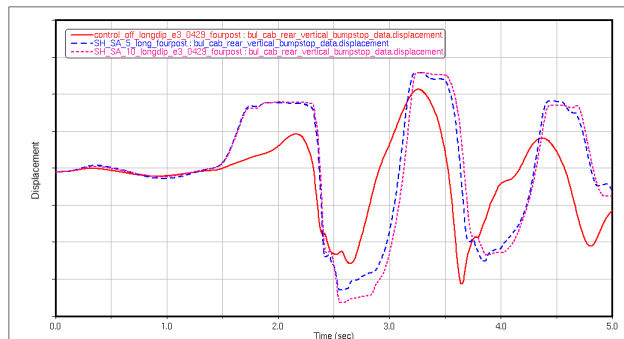
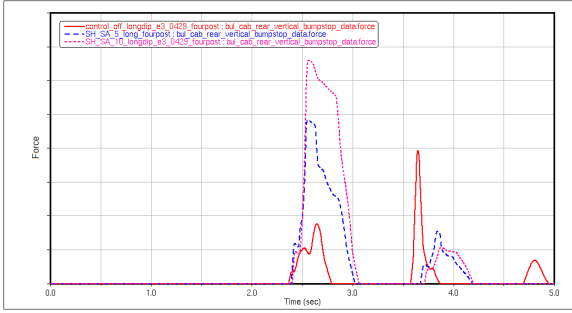
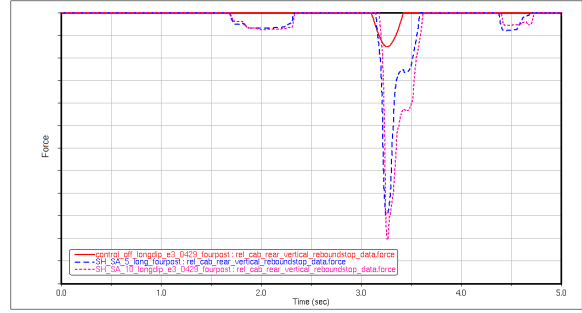


Figure 5.18: Displacements of the bump stop and rebound stop for the benchmark test and for semi-active skyhook control. — Benchmark kNs/m , - - $c_{sky} = 5$ kNs/m , ··· $c_{sky} = 10$ kNs/m



(a) Bump stop forces, rear left hand side



(b) Rebound stop forces, rear left hand side

Figure 5.19: Forces in the a) bump stop and b) rebound stop for the benchmark test and for active skyhook control. — Benchmark kNs/m , - - $c_{sky} = 5 kNs/m$, - - - $c_{sky} = 10 kNs/m$

6 Discussion

This chapter compiles and emphasizes the results of the thesis project and compares the different control systems and strategies to one and other. The system response is evaluated based on the assumptions and the theories upon which the controllers are designed, as well as findings from previous research. Interesting fields for continued research and recommendations for future work is also presented.

6.1 Comparison of active and semi-active control

The active controllers are represented by individual skyhook, modal skyhook and LQR. The semi-active controllers include the different skyhook strategies, i.e. individual and modal control. The best result that is obtained from the different subcases of each control system is compiled in Figure 6.1, which shows how the comfort value is changed compared to the benchmark test for the different road inputs.

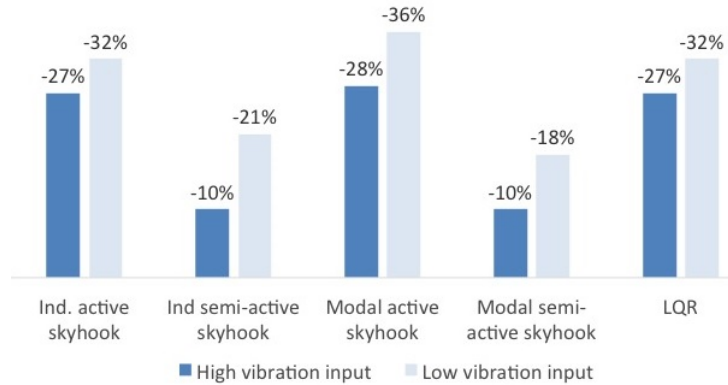


Figure 6.1: *Change of the comfort value for the different control systems and road severities, compared to the benchmark tests*

The results that are obtained with the active systems are consistent with the findings from the literature review [6]. The ride comfort is improved with over 30 % when substituting the conventional passive dampers to active suspensions. This result is obtained for low road vibration input, corresponding to a less maintained road. When the vehicle is traveling on a badly maintained road with high road vibrations, the best result shows an improvement of 20 – 30 %. As expected, the same improvement is not achieved with semi-active systems for which the best result shows a decrease of the comfort value with about 20 % for analysis with low road vibrations. The best results from the analysis with the high road vibrations indicate a possible improvement of about 10 %. One thing that possibly can improve the result for the semi-active controllers is to implement an alternative no-jerk algorithm that can apply forces that are closer to the desired forces.

The handling study shows similar or improved response for both the active and semi-active controllers compared to the conventional suspensions. Active control indicates larger improvements of both the roll and pitch motions compared to semi-active control, as expected. There is a strong correlation between the roll angle and the damping force, which explain why the active system performs better than the semi-active controllers.

It's important to keep in mind that all results are obtained under "ideal" conditions and it is not realistic to presume that the same performance can be achieved in a real truck. In reality, there is a time delay in the control system, i.e. a delay from when the force is desired to when it is actually applied. Also, there are likely to be disturbances in the signal that affects the performance of the control system. Furthermore, the damping force for the semi-active controllers is set to zero when the system is in low state to be as close to the desired force as possible. This can never be achieved with a real semi-active system as the damping characteristics change in real time and the damping coefficient has a nonzero minimum value as well as a maximum value.

6.2 Comparison of individual and modal control

The result from the comfort analysis with the different control strategies indicates that it is possible to achieve better performance with modal control. Most subcases with modal control shows equivalent or improved comfort compared to the cases with individual control, even if the difference is small. However, it is seen that the semi-active modal control switch between high state and low state more frequently, resulting in a jerky system. This induces problems for the solver, which in turn increases the simulation time significantly. This is clearly a disadvantage of the control system, even if it performs well. Note that this problem only occurs for the modal semi-active case. Neither of the control strategies have been optimized to find the optimal damping parameter(s) with respect to comfort. This suggests that especially modal control have great potential for further improvement if the coefficients were tuned more carefully. There is potential for improvement of the individual control too but since c_{sky} is the only variable, it is easier to identify trends in the system behaviour. From the studies made with individual control it is already possible to estimate an optimal value for c_{sky} and the corresponding comfort gain.

The handling analysis shows major similarities regarding the system response; see for example Figure 5.11 that shows the roll angle and damping force for active modal control compared to active individual control. A strong correlation of the roll angle and the applied force is found and it is likely that the curves would coincide if the parameters were tuned differently. The modal skyhook was expected to perform better, especially in terms of roll and pitch motions, since the algorithm targets the different motions of the cab instead of the suspensions velocities. The results could be explained by poorly chosen heave, roll or pitch coefficients.

The relation between the maximum damping force and the overall performance of the different control strategies also shows a strong correlation. This suggests that the system response is highly influenced by the power supply but this is not feasible to conclude from the maximum force only. An alternative would be to look at the RMS values of the applied force or the total work performed by the actuators, which should give more information about the overall power supply. The studies and in particular the studies concerning the modal skyhook control are insufficient for a fair comparison of the different strategies. A more thorough study that comprises optimization of the parameters is necessary to fully evaluate the control strategies.

6.3 Cab model

The cab is modelled using three degrees of freedom (heave, roll and pitch) which are assumed to capture the majority of the behaviour of the cab. Moreover, many features of the cab and its suspensions are neglected, e.g. the stabilizer bar and bushings. The model is further simplified in conjunction with the development of the LQR algorithm, where the motion of the chassis is neglected. All these assumptions and simplifications mean that there is a limited amount of information about the model behaviour. The LQR algorithm would likely be even more efficient if the state space model included more degrees of freedom. Parts that could be incorporated in the model are the chassis, the stabilizer bar, the tyres, the engine etc. With an enhanced cab model it would be possible to design a control system that can address more complex vehicle behaviour. If the chassis is to be modelled, it is necessary to investigate if it possible to model it as flexible part or if a simplified model with a rigid body is sufficient. Another critical part of the modelling concerns the primary suspension that transfers the road vibrations, which is the main vibration source. A control algorithm that can utilize more inputs can also predict the response of the entire truck, not only the cab. A consequence with a more complex model is obviously that it is more difficult to validate the model behaviour.

The simulations point to that it is possible to target the roll and pitch velocities in order to reduce the lateral and the longitudinal accelerations. However, the results are ambiguous and the influence of the roll and pitch angles regarding the horizontal accelerations vary between cases. The front bushings and rear lateral dampers certainly affect the motions of the cab. The translational motions of the cab add to the accelerations of the centre of gravity but without affecting the angular velocities. To better understand the dynamics of the cab, the bushings and lateral dampers should be incorporated in the cab model. Furthermore, the simulations show that close to all of the lateral accelerations can be derived directly from the roll angle. However, the simulations do not show the same correlation between the pitch angle and the longitudinal accelerations, which only partially can be derived from the pitch angle. The vertical acceleration is measured in a point that is influenced by both

heave and the angular velocities and it is therefore more difficult to draw conclusions regarding the vertical motion. The model could also be enhanced to include more degrees of freedom, which would enable to better describe the motions of the cab.

6.4 Road profiles and road obstacles

The control systems have proven to be effective when the truck is operating on a flat road with vibration input but problems occur when there are sudden and larger obstacles in the road. This is seen in long dip analysis, for which the performances of the control systems are poor. The problem occurs as the skyhook control is designed to isolate the cab from any disturbances in the road. For example, when the cab moves downwards in the vertical direction, the control system tries to minimize the motion of the cab and keep the cab in its original vertical position. This results in large damping forces that act between the cab and the chassis. This in turn creates large displacements of the suspension, which engages the bump and rebound stops. The response is improved by softening the suspensions by decreasing c_{sky} but the system still experiences large internal forces. The semi-active control systems perform better but which only is a result of smaller damping forces. Consequently, the algorithm itself proves to be ineffective for this kind of road profile. The same problems that occur for the long dip will occur if the truck travels over a speed bump or a pothole. One possible solution is to use a filter, as the signals corresponding to e.g. slopes or long dips have lower frequencies than road vibrations. The road input will have different frequencies depending on the speed of the truck and a challenge is to define which part of the signal that corresponds to road vibrations. Another solution is to have a control system that behaves differently depending on the road, e.g. flat roads, slopes, pot holes etc. An obvious challenge with this is how the control system should be made aware of the environment in which the vehicle is operating. It becomes clear that the main challenge when designing a control system is to develop a system that can handle all possible road severities, obstacles and manoeuvres.

6.5 Recommendations for future work

To realize the implementation of active or semi-active cab suspension continued and substantial studies are required. First of all, to fully evaluate the control systems and different strategies, it is necessary to conduct an optimization of the damping parameters for each case. Furthermore, the control system must be able to adapt to different road qualities and driving conditions. It is recommended to include more load cases, driving manoeuvres and road input in the analysis to ensure good system response and safety when operating a commercial truck. To achieve this, it is necessary to design a more advanced control algorithm that can handle more inputs.

As this thesis only emphasizes the possibilities with ideal control systems, it is recommended to investigate the system response for a controller with characteristics closer to what actually can be achieved in a real truck. The performance and the stability of the system need to be analysed with disturbances and time delay included. Disturbances in the signal will mainly occur as a result of the accuracy of the sensors. It is recommended to evaluate the system response for random noise and investigate suitable filter functions that can be integrated in the control system. Moreover, the time delay between when the force is desired to when the force is applied should be incorporated in the model of the actuator. With a model that better simulates a real controller, it is possible to evaluate the requirements of the system and the actuators and estimate how these requirements relate to cost.

Since the focus of this thesis mainly was to improve ride comfort when operating a vehicle on a flat road with vibration input it was chosen to only study the vertical dampers. However, it was found that the lateral dampers influence the roll angle of the cab. It would therefore be interesting to design and implement a control system for the lateral dampers as well and study the potential performance gains. The analytical model also has potential for improvement. To consider all forces that act on the cab, the rear lateral dampers and bushings as well as the bump and rebound stop should be incorporated in the model. This would enable better understanding of the dynamics of the cab. Furthermore, to improve the performance of the LQR control in particular, it would be of interest to incorporate more degrees of freedom related to the stabilizer bar, the chassis, the wheel axles etc. in the model as well.

7 Conclusions

The thesis project shows that it is possible to improve ride comfort and handling features of a commercial truck through the use of active and semi-active cab suspensions. This is clearly shown in the comfort analysis where both the vertical, lateral and longitudinal accelerations of the cab are reduced. The active systems show improvements independent of road severity while the semi-active systems mainly perform well for roads with low road vibrations. It is found from studying different control strategies that there are advantages to have a modal approach on the damping control, i.e. design the control based on the motions of the centre of gravity, different from controlling the damping based on the suspension velocities. The handling features are uncompromised or even improved when implementing active or semi-active controllers in the cab suspensions. These results only hold for flat roads and not when the vehicle travels in steep slopes and suddenly changes its vertical position, for which the performance of the control systems is poor. This is seen in simulations where the vehicle is driving through a long dip in the road.

This study mainly points to the characteristic system response pertinent to different control systems and for a limited range of road input and handling manoeuvres. The control algorithms, upon which this project is based, have therefore large potential for further improvement as it is required to have a general control system that performs well independent of the road profiles and vehicle manoeuvres. Moreover, the system response here is ideal, which means that it is not realistic to presume that this result would be obtained in a real truck. Attributes that are not considered here are time delay in the control system and disturbances in the signals. The quality of the result would be improved if models for the sensors and actuators were used. This would show how disturbances, delay and limitations of the hardware affect the system. Further analysis is therefore required and experimental data would be necessary to validate and verify the results. This would also make it possible to determine the requirements for the sensors and actuators as well as the power consumption of the control system.

When addressing the realization of new cab suspension are semi-active dampers the most probable choice. Even if active dampers show a significant improvement are active systems in general larger, far more power consuming and expensive than semi-active systems. It is uncertain if the performance of the semi-active system holds if time delay and signal disturbances were incorporated in the system. To perform well regardless of road input, a more enhanced control system is probably required. Improving the "no-jerk" algorithm, which makes the transition from low state to high state continuous, could be a part of the solution and should be investigated further. Even so, one of the key problems here is how to achieve good performance independent of the road quality, since clearly, it is not acceptable to have a system that only performs well under certain conditions.

The main output of the thesis is a study of active and semi-active cab suspension and a method to design and implement control systems in Adams/Car for complete vehicle analysis. The study satisfies the goals and the purposes that were stated when the project was initiated to a large extent. The thesis project is important for the continued work on improved features of the cab suspensions at Volvo Group Truck Technologies and contributes to present research with various simulations of different road qualities and manoeuvres in combination with a complete vehicle approach.

References

- [1] Karamihas S. Gillespie T. Simplified models for truck dynamic response to road inputs. *International Journal of Heavy Vehicle Systems* **7.1** (2000), p 52–63.
- [2] Spieck M. Krüger W.R. Vaculín O. Semi-Active Suspensions for Road and Off-Road Vehicles - an overview. *Journal of Middle European Construction and Design of Cars* **2** (2004), p 1–14.
- [3] Anthonis J. Baerdemaeker J. Ramon H. Deprez K. Dimitrios D. Improvement of vibrational comfort on agricultural vehicles by passive and semi-active cabin suspensions. *Computers and Electronics in Agriculture* **49.3** (2005), p 431–440.
- [4] Karnopp D. Vibration Control using Semi-active Force Generators. *Journal of Engineering for Industry* **96.2** (1974), p 619–626.
- [5] Van Deussen B.D. Truck suspension system optimization. *Journal of Terramechanics* **9.2** (1973), p 83–100.
- [6] Isermann R. Fischer D. Mechatronic semi-active and active vehicle suspension. *Control Engineering Practice* **12.11** (2004), p 1353–1367.
- [7] Florin M. *Semiactive Cab Suspensions Control for Semitruck Applications*. 2009.
- [8] Jacobsson B. *Vehicle Dynamics, Compendium for Course MMF062*. 2014.
- [9] *Adams Help. Version 2013.2*. Adams.
- [10] Pacejka H.B. *Tyre and vehicle dynamics*. Butterworth-Heinemann, 2002.
- [11] *Cosin.eu [Internet], Cosin scientific software. [cited 2015 February 11]*. URL: http://www.cosin.eu/prod_Ftire.
- [12] Lindström A. *Feature Guideline Ride Comfort and Vibrations, Volvo Group Trucks Technology, Unpublished internal document*.
- [13] International Organization for Standardization. *International Organization for Standardization, Mechanical vibration and shock—evaluation of human exposure to whole body vibration—part 1: general requirements*. ISO 2631-1:1997. 1997.
- [14] Öijer F. *Mathematical Descriptions of Customer Roads with Focus on Long Distance Applications, Volvo Group Trucks Technology, Unpublished internal document*. 2003.
- [15] Evers W.J. *Improving driver comfort in commercial vehicles, Modeling and control of a low-power active cabin suspension system*. 2010.
- [16] Holen P. On modally distributed damping in heavy vehicles. Doctoral thesis in Vehicle Engineering, Department of Aeronautical and Vehicle Engineering, KTH, Stockholm, Sweden (2006).
- [17] Williams D.A. Wright P.G. The application of active suspension to high performance road vehicles. *Proc. IMechE Conf. Microsensors Fluid Power Eng.* (1984), p 23–28.
- [18] Kim M.H. Lee S.R. Bae J.Y. Hwang S.H. Development of semi-independent type continuously variable damper system by performance evaluation of full vehicle test. *International Journal of Vehicle Design* **31.3** (2003), p 269–288.
- [19] Berbyuk V. *Structural Dynamics Control, Chalmers University of Technology, Göteborg*. 2014.
- [20] Ahmadian M. No-jerk skyhook control methods for semiactive suspensions. *Journal of vibrations and acoustics* **162.4** (2004), p 580–584.
- [21] Nayfeh S.A. Zuo L. Low order continuous-time filters for approximation of the ISO 2631-1 human vibration sensitivity weightings. *Journal of Sound and Vibration* **265.10** (2003), p 459–465.
- [22] Anders Lindström. *Senior Vehicle Analyst at Volvo Group Truck Technologies*.
- [23] Escolar Eguia E. Bouchot A. Recherche et simulation de nouvelles technologies pour les suspensions cabine et moteur de poids lourds, Volvo Group Trucks Technology, Unpublished internal document (2014).